IOPscience iopscience.iop.org

Home Search Collections Journals About Contact us My IOPscience

Spin-dependent tunnelling in magnetic tunnel junctions

This article has been downloaded from IOPscience. Please scroll down to see the full text article.

2003 J. Phys.: Condens. Matter 15 R109

(http://iopscience.iop.org/0953-8984/15/4/201)

View the table of contents for this issue, or go to the journal homepage for more

Download details:
IP Address: 171.66.16.119
The article was downloaded on 19/05/2010 at 06:30

Please note that terms and conditions apply.

INSTITUTE OF PHYSICS PUBLISHING JOURNAL OF PHYSICS: CONDENSED MATTER

J. Phys.: Condens. Matter **15** (2003) R109–R142 PII: S0953-8984(03)54596-9

TOPICAL REVIEW

Spin-dependent tunnelling in magnetic tunnel junctions

Evgeny Y Tsymbal[1], **Oleg N Mryasov**[2] **and Patrick R LeClair**[3]

[1] Department of Physics and Astronomy, University of Nebraska-Lincoln, Lincoln, NE 68588, USA
[2] Seagate Research, 1251 Waterfront Place, Pittsburgh, PA 15222, USA
[3] Francis Bitter Magnet Laboratory, Massachusetts Institute of Technology, Cambridge, MA 02139, USA

E-mail: tsymbal@unl.edu

Received 10 October 2002
Published 20 January 2003
Online at stacks.iop.org/JPhysCM/15/R109

Abstract
The phenomenon of electron tunnelling has been known since the advent of quantum mechanics, but continues to enrich our understanding of many fields of physics, as well as creating sub-fields on its own. Spin-dependent tunnelling (SDT) in magnetic tunnel junctions (MTJs) has recently aroused enormous interest and has developed in a vigorous field of research. The large tunnelling magnetoresistance (TMR) observed in MTJs garnered much attention due to possible applications in non-volatile random-access memories and next-generation magnetic field sensors. This led to a number of fundamental questions regarding the phenomenon of SDT. In this review article we present an overview of this field of research. We discuss various factors that control the spin polarization and magnetoresistance in MTJs. Starting from early experiments on SDT and their interpretation, we consider thereafter recent experiments and models which highlight the role of the electronic structure of the ferromagnets, the insulating layer, and the ferromagnet/insulator interfaces. We also discuss the role of disorder in the barrier and in the ferromagnetic electrodes and their influence on TMR.

Contents

1. Introduction 110
2. Early experiments and models 112
  2.1. Experiments on spin-dependent tunnelling 112
  2.2. Stearns' model 114
  2.3. Julliere's experiments and model 115
  2.4. Slonczewski's model 116

0953-8984/03/040109+34$30.00 © 2003 IOP Publishing Ltd Printed in the UK

3. Recent experiments 117
3.1. Magnetic field dependence 118
3.2. Voltage dependence 119
3.3. Temperature dependence 120
3.4. Ferromagnet dependence 121
3.5. Barrier dependence 122
3.6. Interface dependence 124
3.7. Coulomb blockade effects 126
4. Models for perfect junctions 127
4.1. Free-electron models 127
4.2. Bonding at the ferromagnet/insulator interface 128
4.3. First-principles calculations of TMR 130
5. Models for disordered junctions 132
5.1. Contribution of interface states 133
5.2. Effect of disorder in the barrier 134
5.3. TMR at resonant conditions 136
6. Conclusions 136
Acknowledgments 139
References 139

1. Introduction

In the past few years magnetic tunnel junctions (MTJs) have aroused considerable interest due to their potential applications in spin-electronic devices such as magnetic sensors and magnetic random-access memories (MRAMs). The diversity of the physical phenomena which govern functioning of these magnetoresistive devices makes MTJs also very attractive from the fundamental physics point of view. This stimulated tremendous activity in the experimental and theoretical investigations of the electronic, magnetic, and transport properties of MTJs.

A MTJ consists of two ferromagnetic metal layers separated by a thin insulating barrier layer. The insulating layer is so thin (a few nanometres or less) that electrons can tunnel through the barrier if a bias voltage is applied between the two metal electrodes across the insulator. The most important property of a MTJ is that the tunnelling current depends on the relative orientation of the magnetizations of the two ferromagnetic layers, which can be changed by an applied magnetic field. This phenomenon is called tunnelling magnetoresistance (TMR) (sometimes referred to as junction magnetoresistance). Although TMR has been known from the experiments of Julliere [1] for almost 30 years, only a relatively modest number of studies had been performed in this field up to the mid-1990s. Partly this was caused by the technologically demanding fabrication process, which makes it difficult to fabricate robust and reliable tunnel junctions. Also the fact that the reported values of TMR were small (at most a few per cent at low temperatures) meant that no great interest was triggered as regards sensor/memory applications. A few years ago, however, Miyazaki and Tezuka [2] demonstrated the possibility of large values of TMR in MTJs with Al_2O_3 insulating layers, and Moodera *et al* [3] developed a fabrication process which appeared to fulfil the requirements for smooth and pinhole-free Al_2O_3 deposition. Since the first observation of reproducible, large magnetoresistance at room temperature, shown in figure 1, there has been enormous increase in the amount of research in this field. Nowadays MTJs that are based on 3d-metal ferromagnets and Al_2O_3 barriers can be routinely fabricated with reproducible characteristics and with TMR values up to 50% at room temperature, making them suitable for industrial applications (see, e.g., [4]).

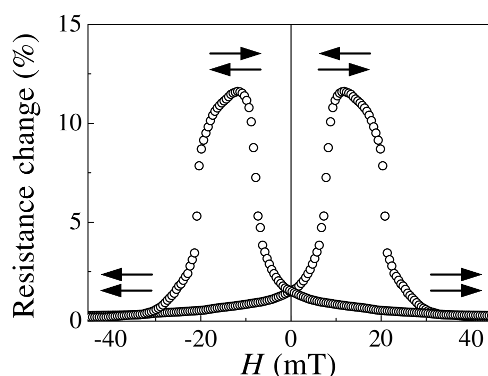

Figure 1. The first observation of reproducible, large room temperature magnetoresistance in a CoFe/Al_2O_3/Co MTJ. The arrows indicate the relative magnetization orientation in the CoFe and Co layers (after [3]).

TMR is a consequence of spin-dependent tunnelling (SDT). The essence of SDT is an imbalance in the electric current carried by up- and down-spin electrons tunnelling from a ferromagnet through a tunnelling barrier. The origin of this phenomenon can be explained by the fact that the probability for an electron to tunnel through the barrier depends on its Fermi wavevector. In ferromagnetic metals electronic bands are exchange split, which implies different Fermi wavevectors for the up- and down-spin electrons and consequently a tunnelling probability that depends on spin. The SDT effect was discovered in pioneering experiments by Tedrow and Meservey [5]. Using superconducting layers as detectors they measured the spin polarization of the tunnelling current originating from various magnetic electrodes across an alumina barrier. An excellent review on SDT was published by Meservey and Tedrow [6], which covers the field up to 1994.

The relationship between SDT and TMR was explained by Julliere within a simple model [1] that quantifies the magnitude of TMR in terms of the spin polarizations (SP) of the ferromagnetic electrodes as measured in the experiments on superconductors [5]. Although Julliere's model served as a useful basis for interpreting a number of experiments on TMR, this model is too simple to describe all the available experimental data. In particular, Julliere's model assumes that the SP of the tunnelling current is determined solely by the SP of the total electronic density of states (DOS) of the ferromagnetic layers at the Fermi energy. Although later Stearns improved this understanding by considering only the DOS of itinerant electrons [7], the interpretation of TMR in terms of the intrinsic properties of the ferromagnets constituting the MTJ remained unchanged. Experimental results show, however, that the tunnelling SP strongly depends on the structural quality of MTJs. Improvements in the quality of the alumina barrier and the metal/alumina interfaces resulted in the enhancement of the measured values of the SP. For example, the SP of permalloy of 32% was obtained in first experiments on tunnelling to superconductors [6], but later Moodera *et al* using improved deposition techniques reported the value of 48% (see [8]). Experiments also show that the SP depends on the choice of the tunnelling barrier. Fert and his group found that Co exhibits a negative value of the SP when tunnelling occurs through a $SrTiO_3$ barrier [9]. This is opposite to the spin polarization of tunnelling electrons across an Al_2O_3 barrier, for which all 3d ferromagnets show positive SP [6]. Also recent experiments by LeClair *et al* [10–12] demonstrated the decisive role of the electronic structure of the interfaces in SDT.

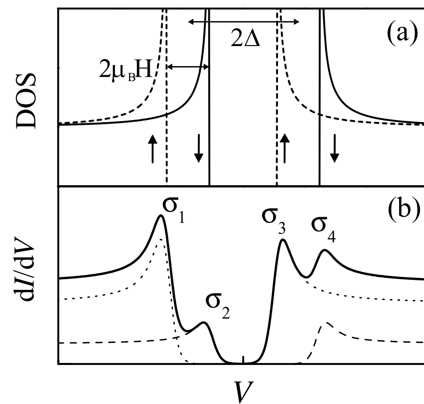

Figure 2. Tunnelling in a ferromagnet/insulator/superconductor junction. (a) The DOS of the superconductor split by a value of $2\mu_B H$ into the up- and down-spin contributions. (b) Conductance as a function of voltage for each spin orientation (dotted and dashed curves) and the total conductance (solid curve) (after [6]).

It is evident, therefore, that the tunnelling SP is *not* an intrinsic property of the ferromagnet alone but depends on the structural and electronic properties of the entire junction including the insulator and the ferromagnet/insulator interfaces. This fact makes the quantitative description of transport characteristics of MTJs much more complicated; however, it broadens dramatically the possibilities for altering the properties of MTJs. In particular, by modifying the electronic properties of the tunnelling barrier and the ferromagnet/insulator interfaces it is possible to engineer MTJs with properties desirable for device applications.

The main objective of this review article is to address various factors that control the magnitude of magnetoresistance in MTJs. Starting from early experiments on SDT and their interpretation, we consider then recent experiments and models, which highlight the role of the electronic structure of the ferromagnets, the insulating layer, and the ferromagnet/insulator interfaces. We also discuss the role of disorder in the barrier and in the ferromagnets and their influence on magnetoresistance.

The most recent reviews on SDT by Levy and Zhang [13] and by Moodera *et al* [8] appeared in 1999 and summarized experimental and theoretical results published up to that date.

2. Early experiments and models

2.1. Experiments on spin-dependent tunnelling

The field of SDT was founded by the pioneering experiments of Tedrow and Meservey [5, 6]. They used ferromagnet/insulator/superconductor (FM/I/S) tunnel junctions to measure the spin polarization of the tunnelling current originating from various ferromagnetic metals across an alumina insulating barrier. In these experiments, electrons tunnel through the barrier to a superconducting Al film which acts as a spin detector. The superconducting DOS has a gap of 2Δ in the quasiparticle spectrum and characteristic singularities at $E = \pm\Delta$. If the thin superconducting film (a few nanometres or less) is placed in a magnetic field $\boldsymbol{H}$ applied parallel (subscript P) to the film plane, the quasiparticle states in the superconductor split due to the Zeeman interaction of the magnetic field with the electron spin magnetic moment. In this case, the DOS of the superconductor is the superposition of the up- and down-spin contributions separated by energy of $2\mu_B H$, as shown in figure 2(a). The orientation of the magnetic moment and therefore the spin directions are defined by the applied field.

The sharply peaked DOS of the superconductor makes it possible to separate the contributions from the up- and down-spin electrons in the tunnelling current. As a result,

Table 1. Tunnelling SP obtained in experiments on FM/Al_2O_3/Al tunnel junctions.

FM	Ni	Co	Fe	$Ni_{80}Fe_{20}$	$Ni_{40}Fe_{60}$	$Co_{50}Fe_{50}$	$Co_{84}Fe_{16}$
P (%), old values [6]	23	35	40	32	—	—	—
P (%), new values [8, 14]	33	42	45	48	55	55	55

tunnelling from a ferromagnetic metal into such a superconductor gives rise to an asymmetric conductance curve, which is schematically shown in figure 2(b). This asymmetry is the consequence of the fact that electronic states in the ferromagnetic metal are exchange split, which leads to an unequal DOS in the ferromagnet at the Fermi energy, $\rho^{\uparrow} \neq \rho^{\downarrow}$. Since $\rho^{\uparrow}$ and $\rho^{\downarrow}$ determine the number of electrons which can tunnel within each spin channel, the spin conductance is weighted with the respective spin DOS. Assuming that spin does not change in the tunnelling process, i.e. the total conductance is the sum over the up- and down-spin channels, $G = G^{\uparrow} + G^{\downarrow}$, the tunnelling spin polarization can be obtained by measuring the relative heights of the conductance peaks displayed in figure 1:

$$P = \frac{G^{\uparrow} - G^{\downarrow}}{G^{\uparrow} + G^{\downarrow}} = \frac{(\sigma_4 - \sigma_2) - (\sigma_1 - \sigma_3)}{(\sigma_4 - \sigma_2) + (\sigma_1 - \sigma_3)}. \quad (1)$$

A more accurate determination of the tunnelling spin polarization in FM/I/S junctions must account for spin–orbit scattering in the superconductor [6, 8]. Table 1 shows the experimental values of the spin polarization of the tunnelling current across Al_2O_3 into superconducting Al from various ferromagnetic 3d metals corrected for the spin–orbit scattering. Along with the values of P obtained in early experiments [6], recently measured values are shown in table 1. These new values of the spin polarization are higher than the old ones due to improved deposition techniques resulting in cleaner junctions with better interfaces.

We note here that although the relatively recent technique of Andreev reflection [15] is also capable of measuring spin polarization, its relevance for MTJs and TMR values is questionable at best. Andreev reflection weights the contribution of different electronic states differently to tunnelling, and further, the influence of the insulating barrier implicit in the tunnelling process is not present. Thus, although there does seem to be a rough correspondence between SDT across Al_2O_3 and Andreev reflection measurements, this correspondence is most probably spurious.

The results of these early experiments on SDT were interpreted in terms of the DOS of the ferromagnetic electrodes at the Fermi energy. Assuming that the spin conductance is proportional to $\rho^{\uparrow}$ for the majority-spin electrons and is proportional to $\rho^{\downarrow}$ for the minority-spin electrons, we arrive at the result that the measured values of the SP of the tunnelling conductance, P, should be equal to the SP of the DOS at the Fermi energy of the ferromagnet:

$$P_{FM} = \frac{\rho^{\uparrow} - \rho^{\downarrow}}{\rho^{\uparrow} + \rho^{\downarrow}}. \quad (2)$$

This result demonstrates, however, inconsistency between the measured and predicted values of the SP. Indeed, as is evident from table 1, the SP of the tunnelling conductance from all the 3d ferromagnetic metals and their alloys appears to be positive, which implies that the majority-spin electrons tunnel more efficiently than the minority-spin electrons. This is in contradiction with the bulk band structure, at least for the two ferromagnetic metals, Co and Ni, which make the dominant contribution of the minority spins at the Fermi energy, making the respective SP of the DOS negative.

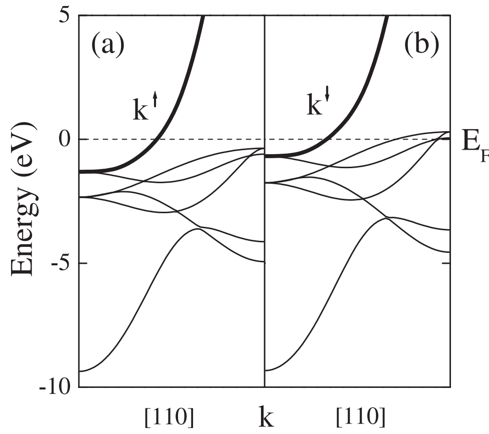

Figure 3. Electronic bands in bulk fcc Ni in the [110] direction for the majority-spin (a) and minority-spin (b) electrons. The heavy curves show the free-electron-like bands which dominate tunnelling. $k^{\uparrow}$ and $k^{\downarrow}$ are the Fermi wavevectors which determine the spin polarization of the tunnelling current (after [7]).

2.2. Stearns' model

This inconsistency between the experimental and theoretical values of the SP is the consequence of the fact that the tunnelling conductance depends not only on the number of electrons at the Fermi energy but also on the tunnelling probability, which is different for various electronic states in the ferromagnet. The electronic structure of the 3d ferromagnets is characterized by dispersive s bands, which are hybridized with more localized d bands. The latter have a strong weight at the Fermi energy for the minority-spin electrons in Co and Ni that leads to the negative SP of the DOS in these ferromagnets. These features of the electronic band structure were taken into account by Stearns [7], who developed a simple quantitative model to treat the spin polarization of electrons tunnelling from various ferromagnetic metals. Stearns pointed out that the transmission probability depends on the effective mass which is different for different bands. The localized d electrons have a large effective mass and therefore decay very rapidly into the barrier region, whereas the dispersive s-like electrons decay slowly. According to this argument, the nearly free-electron, most dispersive bands should provide essentially all the tunnelling current[4].

Stearns' idea is illustrated in figure 3, which shows the electronic bands of bulk Ni in the [110] direction. As is seen from this figure, for the majority-spin electrons the dispersive s band is the only one that crosses the Fermi energy (figure 3(a)). For the minority spins, however, there are several bands that appear at the Fermi level (figure 3(b)). According to Stearns' argument, the dispersive band that is indicated in figure 3(b) by the heavy solid curve is the only band contributing to the tunnelling process—the other localized bands are essentially to be disregarded.

The dispersive bands that dominate tunnelling are similar to free-electron bands, and, therefore, the DOS of these bands at the Fermi energy is proportional to their Fermi wavevector. Assuming that the conductance is proportional to the DOS of these itinerant electrons we can rewrite equation (2) for the SP of the ferromagnet as

$$P_{FM} = \frac{k^{\uparrow} - k^{\downarrow}}{k^{\uparrow} + k^{\downarrow}}, \tag{3}$$

where $k^{\uparrow}$ and $k^{\downarrow}$ are the Fermi wavevectors of the dispersive bands for the majority and minority spins. Using an accurate analysis of the electronic band structure, Stearns found that $P_{FM} = 45\%$ for Fe and 10% for Ni, which are consistent with the experimental data.

[4] Note that Stearns designates these bands as 'itinerant d electrons'.

Stearns actually introduced a notion of 'tunnelling density of states'. This notion was used by other researchers (e.g., [16]) to designate the effective number of electrons which can tunnel from one ferromagnetic metal and the number of effective empty states available in the other ferromagnetic metal, so the tunnelling conductance per spin is proportional to their product. In the model proposed by Stearns, the tunnelling DOS is identified as the Fermi wavevectors of the itinerant electrons with corresponding spin. The results obtained by Stearns are an early indication of the fact that the understanding of SDT requires a detailed knowledge of the electronic structure of MTJs.

2.3. Julliere's experiments and model

An important advance was made by Julliere [1] in 1975, a few years later after the successful experiments on SDT were reported. In these experiments the superconducting film was replaced by another ferromagnetic metal film, thereby making a FM/I/FM tunnel junction. It was reasoned that instead of using magnetic-field-induced spin-split states of a superconductor as a spin detector it is possible to use exchange-split states of another ferromagnet. In this case, it was expected that the tunnelling current should depend on the relative magnetization orientation of the two ferromagnetic electrodes, giving rise to TMR. This is in fact what was observed. Using Co and Fe ferromagnetic films with different coercive fields and a Ge barrier layer, Julliere observed sizable magnetoresistance at 4.2 K. The maximum TMR value was found to be about 14% at zero bias, but decreased very rapidly with increasing bias voltage, as shown in figure 4. This rapid decrease in TMR was attributed to spin-flip scattering at ferromagnet/barrier interfaces.

Julliere interpreted these results in terms of a simple model, which is based on two assumptions. First, he assumed that spin of electrons is conserved in the tunnelling process. It follows, then, that tunnellings of up- and down-spin electrons are two independent processes, so the conductance occurs in the two independent spin channels. Such a two-current model is also used to interpret the closely related phenomenon of giant magnetoresistance (GMR) (see, e.g., [17]). According to this assumption, electrons originating from one spin state of the first ferromagnetic film are accepted by unfilled states of the same spin of the second film. If the two ferromagnetic films are magnetized parallel, the minority spins tunnel to the minority states and the majority spins tunnel to the majority states. If, however, the two films are magnetized antiparallel (subscript AP) the identity of the majority- and minority-spin electrons is reversed, so the majority spins of the first film tunnel to the minority states in the second film and vice versa. Second, Julliere assumed that the conductance for a particular spin orientation is proportional to the product of the effective (tunnelling) DOS of the two ferromagnetic electrodes. According to these assumptions, the conductance for the parallel and antiparallel alignment, G_P and G_{AP}, can be written as follows:

$$G_P \propto \rho_1^{\uparrow}\rho_2^{\uparrow} + \rho_1^{\downarrow}\rho_2^{\downarrow}, \tag{4}$$

$$G_{AP} \propto \rho_1^{\uparrow}\rho_2^{\downarrow} + \rho_1^{\downarrow}\rho_2^{\uparrow}, \tag{5}$$

where $\rho_i^{\uparrow}$ and $\rho_i^{\downarrow}$ are the tunnelling DOS of the ferromagnetic electrodes (designated by index $i = 1, 2$) for the majority- and minority-spin electrons. It follows from equations (4) and (5) that the parallel- and antiparallel-magnetized MTJs have different conductances, which implies a non-zero TMR. We define TMR (following the majority of researchers) as the conductance difference between parallel and antiparallel magnetizations, normalized by the antiparallel conductance, i.e.

$$\mathrm{TMR} \equiv \frac{G_P - G_{AP}}{G_{AP}} = \frac{R_{AP} - R_P}{R_P}. \tag{6}$$

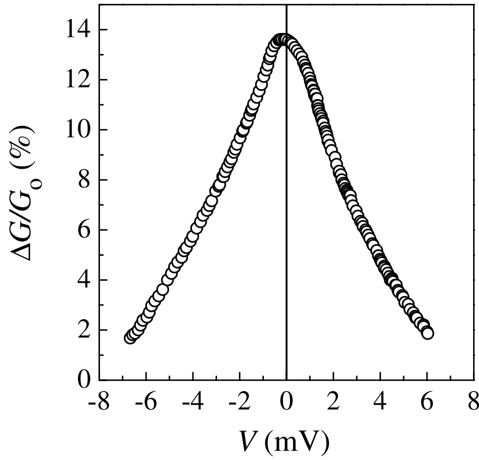

Figure 4. The original demonstration of the TMR effect. The relative conductance change due to an applied magnetic field versus applied bias in a Fe/Ge/Co junction at 4.2 K (after [1]).

Using equations (4) and (5), we arrive then at Julliere's formula:

$$\mathrm{TMR} = \frac{2P_1P_2}{1 - P_1P_2}, \tag{7}$$

which expresses the TMR in terms of the effective SP of the two ferromagnetic electrodes:

$$P_i = \frac{\rho_i^{\uparrow} - \rho_i^{\downarrow}}{\rho_i^{\uparrow} + \rho_i^{\downarrow}}, \tag{8}$$

where $i = 1, 2$. Using the known values of the spin polarization for Co and Fe from experiments of Tedrow and Meservey [5], Julliere deduced the TMR value of 26%, which is larger than the maximum measured value of 14%. He explained the discrepancy by magnetic coupling between the ferromagnetic electrodes and spin-flip scattering.

These results of Julliere stimulated further research in the field of MTJs. Unfortunately, they were not reproduced by other researchers, and their true interpretation is still the subject of debate. Nevertheless, the importance of the paper by Julliere should not be underestimated—in particular, his simple quantitative model which was later used by many researchers to correlate the magnitude of TMR in MTJs with the SP of ferromagnets measured in experiments on FM/I/S tunnel junctions.

2.4. Slonczewski's model

The first accurate theoretical consideration of TMR was made by Slonczewski [18]. He considered tunnelling between two identical ferromagnetic electrodes separated by a rectangular potential barrier assuming that the ferromagnets can be described by two parabolic bands shifted rigidly with respect to one another to model the exchange splitting of the spin bands. Having imposed perfect translational symmetry of the tunnel junction along the layers and matched the wavefunctions of electrons across the junction, he solved the Schrödinger equation and determined the conductance as a function of the relative magnetization alignment of the two ferromagnetic films. In the limit of thick barrier, he found that the conductance is a linear function of the cosine of angle Θ between the magnetic moments of the films:

$$G(\Theta) = G_0(1 + P^2 \cos\Theta). \tag{9}$$

Here P is the effective spin polarization of tunnelling electrons given by

$$P = \frac{k^{\uparrow} - k^{\downarrow}}{k^{\uparrow} + k^{\downarrow}} \frac{\kappa^2 - k^{\uparrow}k^{\downarrow}}{\kappa^2 + k^{\uparrow}k^{\downarrow}}, \tag{10}$$

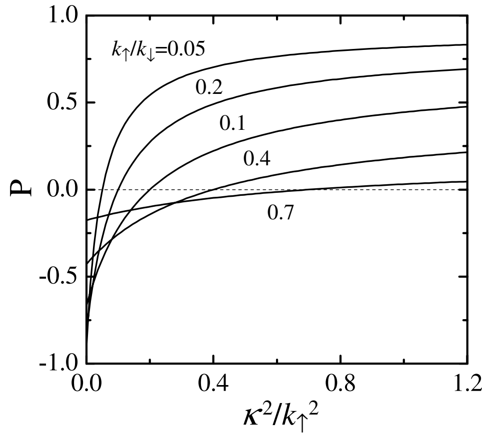

Figure 5. Spin polarization of the tunnelling conductance as a function of the normalized potential barrier height for various values of $k_\uparrow/k_\downarrow$ (after [18]).

where κ is the constant of decay of the wavefunction into the barrier which is determined by the potential barrier height U, $\kappa = \sqrt{(2m/\hbar^2)(U - E_F)}$. As follows from equation (10), in addition to the factor that represents the spin polarization P_{FM} of the ferromagnet (3), the SP of the tunnelling current contains a factor which depends on the barrier height. In the limit of a high barrier it tends to unity, reducing Slonczewski's result for TMR to Julliere's formula. However, if the barrier is not very high and the decay constant is comparable to or less than the wavevectors of electrons in the ferromagnetic metals, the magnitude of the TMR decreases with decreasing U and even changes sign for sufficiently low barriers, which is demonstrated in figure 5.

Slonczewski wrote that these 'results contradict the plausible notion that the spin polarization P is characteristic of the electron structure of the electrode *alone* and would have the same value (sign at least) in any tunnelling experiment'. This was the first important indication of the fact that the SP of the conductance is not an intrinsic property of the ferromagnets.

3. Recent experiments

Over the next two decades, several groups attempted to perform experiments on MTJs using different ferromagnetic electrodes and barrier layers (e.g. [16, 19–23]). In all cases, the observed TMR values were at most a few per cent at relatively low temperatures. In particular, Maekawa and Gäfvert [16] used Ni/NiO/Co junctions to study TMR and to correlate it with the magnetization loops of the ferromagnetic electrodes. They found TMR values of about 2% at 4.2 K, which rapidly decreased with increasing temperature. Although these values were much less than those anticipated, this work clearly indicated that the conductance variation as a function of applied magnetic field was indeed due to the change in the relative magnetization alignment of the two ferromagnetic films.

Only in 1995, nearly 20 years after the first experiments on TMR, did Miyazaki and Tezuka [2] and Moodera *et al* [3] independently demonstrate >10% TMR at room temperature. In the both experiments MTJs based on alumina as a barrier layer separating transition-metal electrodes were used. The results of Moodera *et al* for the resistance change in a CoFe/Al_2O_3/Co MTJ as a function of applied magnetic field are shown in figure 1. The latter experiments demonstrated the fabrication procedure which provides MTJs with a pinhole-free Al_2O_3 tunnel barrier and with smooth interfaces resulting in reproducible, high TMR values at

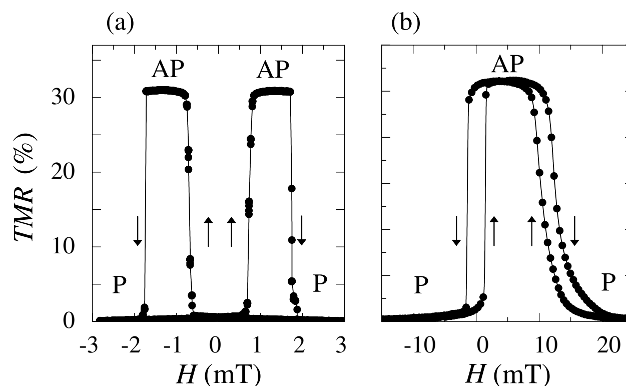

Figure 6. Magnetoresistance versus magnetic field for a hard–soft MTJ (a) and an exchange-biased MTJ (b), both at 10 K. Vertical arrows refer to sweep direction. Both curves are taken at $V = 0$ (from [27]).

room temperature. These achievements quickly garnered a great deal of attention, and catalysed many groups to investigate MTJs. In the next few sections, we discuss most important features of TMR observed experimentally, in particular, the dependence of TMR on magnetic field, bias voltage, and temperature, on the type of the ferromagnet and its crystallographic orientation, on the barrier material and interface properties.

3.1. Magnetic field dependence

In order to observe the TMR phenomenon one needs to realize experimentally both parallel and antiparallel magnetization alignment in a MTJ. Perhaps the simplest way to provide this is to use two ferromagnetic layers with different coercive fields, for example, hard and soft ferromagnets such as Co (hard) and $Ni_{80}Fe_{20}$ (soft). The typical behaviour of TMR versus magnetic field is shown in figure 6(a) for a $Ni_{80}Fe_{20}/Al_2O_3/Co$ junction. When the field is swept through zero and reaches values between the $Ni_{80}Fe_{20}$ and Co coercive fields, an antiparallel magnetization alignment is reached between ± 0.5 and 1.5 mT.

Exchange biasing is another way to realize the parallel and antiparallel magnetization alignment. In this case, one of the magnetic electrodes is in direct contact with an antiferromagnetic (AFM) material (e.g., FeMn or NiO). The presence of an exchange anisotropy at the FM/AFM interface shifts the entire magnetization loop away from zero field, such that it is centred at a finite magnetic field [24]. Typical TMR behaviour for an exchange-biased system is displayed in figure 6(b). Technologically, exchange biasing is advantageous because the resistance transition takes place near zero magnetic field, and it generally results in greater magnetic stability, which is important for technological applications of MTJs [25, 26].

According to Slonczewski's model (section 3.4) a MTJ should work as a spin polarizer of the electric current if the magnetization of one ferromagnetic film rotates with respect to the magnetization of the other. Indeed, the predicted cosine variation of the TMR was found in the experiments by Moodera and Kinder [28]. Using electrodes with different coercive fields they measured the angular dependence of the magnetoresistance, which is shown in figure 7. At a field higher than the coercive field of one electrode, the magnetization of the softer film follows the field direction when the sample is rotated. This gradually changes the relative magnetization orientation of the two ferromagnetic films from parallel to antiparallel. It was found that the resistance variation follows the $\cos\Theta$ dependence, thereby supporting the

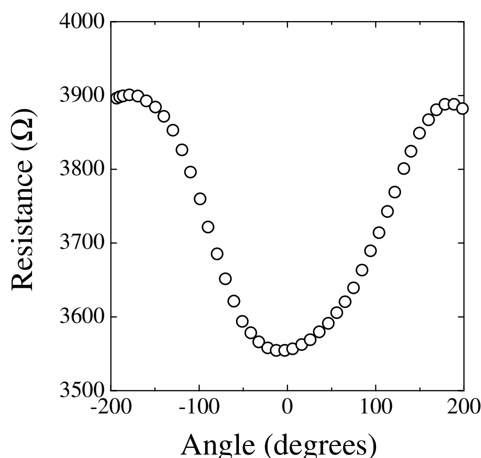

Figure 7. The angular dependence of the magnetoresistance of a CoFe/Al_2O_3/Co junction measured in a magnetic field lower than the coercive field of one electrode but higher than the coercive field of the other electrode (after [28]).

FM/I/FM tunnelling model[5]. When similar measurements were done at a field value higher than the coercive field of both electrodes, no resistance change was found.

3.2. Voltage dependence

In most MTJs the magnitude of the TMR decreases strongly with increasing bias voltage, similarly to that observed originally by Julliere (see figure 4). The figure of merit is the voltage at which the TMR is reduced by a factor of two. In the work of Julliere, only 3 mV bias was needed to halve the TMR value (figure 4). Later Moodera *et al* [3] fabricated junctions with a 'half-voltage' of 200 mV. With improving control of the barriers, several groups increased this value up to more than 500 mV (e.g., [29, 30]).

In order to explain this drop in TMR with bias, Zhang *et al* [31] proposed a model suggesting that inelastic scattering by magnon excitations at the ferromagnet/insulator interface controls the voltage dependence. In the presence of non-zero bias, electrons which have tunnelled across the barrier arrive at the second ferromagnet as hot electrons with energy higher than the Fermi energy of this electrode (provided that no inelastic scattering event has occurred). These hot electrons may then lose their energy by emitting a magnon and thereby flipping the electron spin. With increasing bias voltage more magnons can be emitted, resulting in the reduced TMR values. By using one parameter, in addition to parameters that fix the response at zero bias, Zhang *et al* explained the softening of the TMR with bias up to 200 mV. Later, this model was used by Han *et al* [32], who have performed a careful analysis of the conductance and magnetoresistance as a function of voltage and temperature for $Co_{75}Fe_{25}/Al_2O_3/Co_{75}Fe_{25}$ tunnel junctions.

Although these results and also experiments by Moodera *et al* [33] suggest that the bias dependence of TMR is due to magnon excitations at the interface, recent experiments by Wulfhekel *et al* [34] seem to be inconsistent with this plausible explanation. Using spin-polarized tunnelling microscopy on Co(0001) they studied TMR in a 'MTJ' in which vacuum served as a barrier separating a ferromagnetic STM tip and the Co electrode. Unlike the oxide barriers used in normal MTJs, the barrier in these experiments was 'perfect' and did not suffer

[5] We note that Slonczewski's model predicts the $\cos\Theta$ variation of the *conductance*, whereas the experiments of [28] found the $\cos\Theta$ variation of the *resistance*. The difference between these two dependences is, however, second order in the TMR ratio, and may be sizable only if the resistance change becomes comparable with the resistance itself, which is not the case in [28].

from any imperfections of the oxide. On the other hand, magnon excitations at the interfaces (surfaces of the ferromagnets) could be present. Wulfhekel *et al* found, in sharp contrast to the case for the FM/Al_2O_3/FM junctions, no variation in TMR up to ± 0.9 V at relatively large separations between the ferromagnetic tip and the Co surface. They concluded that most of the voltage dependence is not related to magnon excitations at the interface and put forward a model of Zhang and White [35] who had suggested that the voltage drop in TMR is due to localized trap states in the amorphous barrier. The impurity-assisted contribution to the bias dependence of TMR is also supported by experiments of Jansen and Moodera [36]. Interestingly, the latter mechanism can even result in an *increased* TMR relative to pure junctions, as demonstrated by Jansen and Moodera for Fe-doped NiFe/Al_2O_3/CoFe junctions [37].

Another mechanism which could contribute to the voltage dependence of the conductance and TMR is related to the electronic structure of the ferromagnets. Biasing a MTJ leads to the contribution from electrons which tunnel from the occupied states below the Fermi energy of one electrode to the empty states above the Fermi energy of the other electrode. Due to the change in the electronic structure of the ferromagnets (e.g., the DOS) as a function of energy, the conductance should be energy dependent resulting in the variation of TMR versus the applied voltage. This mechanism should obviously be sensitive to the type of ferromagnet. Surprisingly, however, for the alumina-based MTJs with different ferromagnetic electrodes, band structure effects in the voltage dependence have not been reported until recently. Only recently, using Co/Al_2O_3/Co MTJs with fcc and hcp Co electrodes, have LeClair *et al* [38] found a relationship between the magnetotransport properties and the calculated DOS for the two different crystalline phases of Co. The influence of the electronic structure on the voltage dependence of TMR for MTJs with insulators different from alumina was found in [9, 39] and will be discussed in section 3.5.

3.3. Temperature dependence

In all tunnel junctions the TMR decreases with increasing temperature. As was first noticed by Shang *et al* [40], the temperature dependence of the tunnel resistance for MTJs greatly exceeds that for non-magnetic junctions with nominally identical barriers. Typically, Al/Al_2O_3/Al junctions showed only a 5–10% change in resistance from 4.2 to 300 K, while MTJs always exhibited a 15–25% change in resistance, as shown in figure 8 for a Co/Al_2O_3/Co junction. The TMR can decrease by as much as 25% or more from 4.2 to 300 K depending on the magnetic electrodes. Shang *et al* explained these results within a simple phenomenological model, in which they assumed that the tunnelling spin polarization P decreases with increasing temperature due to spin-wave excitations, as does the surface magnetization. They thus assumed that the tunnelling spin polarization and the interface magnetization followed the same temperature dependence, the well-known Bloch $T^{3/2}$-law, $M(T) = M(0)(1 - \alpha T^{3/2})$. By fitting parameter α, Shang *et al* obtained a satisfactory explanation for the temperature dependence of TMR, as demonstrated by the fit in figure 8(a). MacDonald *et al* [41] provided a more rigorous theoretical justification of these ideas, essentially reproducing the proportionality between $M(T)$ and $P(T)$.

Another mechanism which can cause the reduction of TMR with temperature is spin-flip scattering by magnetic impurities in the barrier. As was shown by Vedyayev *et al* [42], the number of electrons contributing to this process increases with increasing temperature, resulting in the drop of TMR. In addition, inelastic scattering which does *not* flip the spin, such as electron–phonon scattering, can also cause the reduction of TMR in the presence of localized states in the barrier. This was recently demonstrated by Tsymbal *et al* [43], who considered spin-dependent transport across an amorphous barrier, and showed that spin-conserving inelastic scattering is detrimental to TMR.

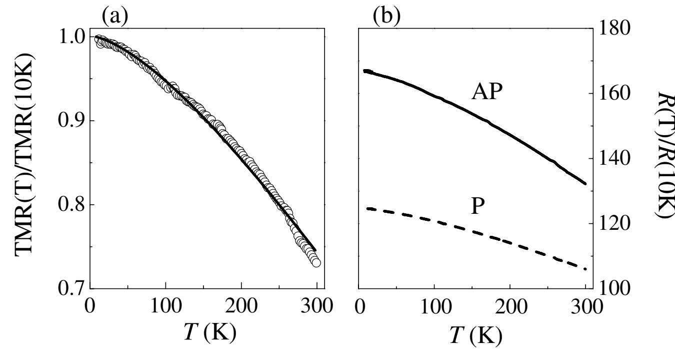

Figure 8. (a) The temperature dependence of TMR for a $Co/Al_2O_3/Co$ MTJ (circles) along with a fit to the model of Shang *et al* [40] (curve). (b) Resistance versus temperature for parallel ('P', dashed curve) and antiparallel ('AP', solid curve) magnetization alignment for the same junction (from [27]).

3.4. Ferromagnet dependence

In general, the most recent spin polarization values with Al_2O_3 barriers obtained via the SDT technique [8, 14] agree well with the maximum TMR values reported with Al_2O_3 barriers [8, 44] within Julliere's model. Table 2 compares the expected TMR values based on Julliere's model, using values of SP obtained from SDT experiments, with TMR values measured using the *same* barriers in both cases. However, we caution that Julliere's model is only a phenomenological guide for estimating the magnitude of the TMR effect when tunnelling SP are known.

Obviously, one expects the largest TMR values for materials with the largest tunnelling spin polarization. This explains a great deal of the recent interest in so-called 'half-metallic' ferromagnets, materials for which only one spin band is occupied at the Fermi level, resulting in perfect 100% spin polarization [46]. Many compounds have been predicted to be half-metallic, such as the half- and full-Heusler alloys NiMnSb [47] and Co_2MnSi [48]; the oxides CrO_2 [49], Fe_3O_4 [50, 51], and $La_{0.67}Sr_{0.33}MnO_3$ (LSMO) [52, 53]; and the sulfide $Co_xFe_{1-x}S_2$ [54]. However, only for LSMO [55], NiMnSb [56], and CrO_2 [57, 58] is there any experimental evidence in favour of half-metallic behaviour. LSMO has been successfully used as electrodes in MTJs by Lu *et al* [59] and Viret *et al* [60], who observed TMR effects of more than 400% at low temperature utilizing $SrTiO_3$, $PrBaCu_{2.8}Ga_{0.2}O_7$, or CeO_2 barriers. Using equation (7), this implies a spin polarization of more than 80%, in agreement with SDT experiments [61]. Sun [62] has also very recently reported more than 100% TMR as well in LSMO/$SrTiO_3$/LSMO junctions. Similarly, Jo *et al* [63] have used another mixed-valence manganite, $La_{0.7}Ca_{0.3}MnO_3$ (LCMO), and investigated LCMO/$NdGaO_3$/LCMO and LCMO/$NdGaO_3$/LSMO MTJs, also observing more than 400% TMR. More recently, Bowen *et al* [45] have observed 1800% TMR in LSMO/$SrTiO_3$/LSMO junctions, implying a spin polarization of 95% based on Julliere's model and essentially corroborating photoemission results showing LSMO to be half-metallic. An extensive review of the magnetotransport phenomenon in magnetic oxides can be found in [64].

Given the expected dependence of TMR on the electronic structure of ferromagnetic electrodes, one would anticipate a dependence on the crystallographic orientation of the electrodes. However, MTJs with even a single epitaxial layer are notoriously difficult to fabricate, and only recently have semi-epitaxial (i.e., with one epitaxial electrode) MTJs been grown. Yuasa *et al* [65] have prepared Fe(100, 110, 211)/Al_2O_3/CoFe MTJs with the epitaxial bottom

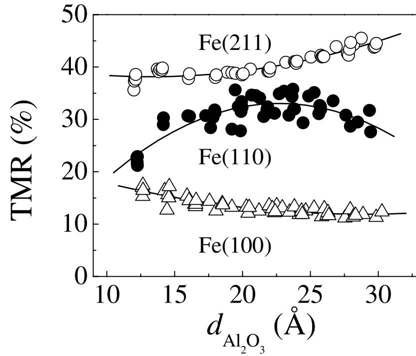

Figure 9. TMR at 2 K as a function of Al_2O_3 thickness for Fe(211), Fe(110), and Fe(100) epitaxial electrodes in Fe/Al_2O_3/CoFe junctions. Curves are only a guide to the eye (from [65]).

Table 2. Comparison of TMR values expected from Julliere's model (using SP data obtained via the Meservey–Tedrow technique) with measured low-temperature TMR values, in each case using the same tunnel barrier.

Junction	TMR (%)		Reference
	Julliere	Experiment	
Ni/Al_2O_3/Ni	25	23	[27]
Co/Al_2O_3/Co	42	37	[27]
$Co_{75}Fe_{25}$/Al_2O_3/$Co_{75}Fe_{25}$	67–74	69	[44]
LSMO/$SrTiO_3$/LSMO	310	1800	[45]

Fe layer to study the effect of the Fermi surface anisotropy on transport properties. They observed a strong dependence of the TMR on crystallographic orientation, as shown in figure 9. This fact clearly points to the details of the Fe band structure [66] and momentum filtering. Naively looking at the most dispersive s-like bands near E_F in Fe [66], the trend TMR[Fe(211)] > TMR[Fe(110)] > TMR[Fe(100)] can perhaps be explained in some way, though, as we will see in section 4.3, it is expected that the Fe(100) tunnelling spin polarization should be much larger. Another possible reason for the dependence of the TMR on crystallographic orientation could be a slightly different growth mode of the amorphous Al_2O_3 on the different crystalline facets of Fe, giving rise to a slightly different barrier quality for each electrode orientation and barrier thickness. However, there is no direct evidence for this mechanism.

3.5. Barrier dependence

Work to date on MTJs has focused almost exclusively on Al_2O_3 tunnel barriers, for a variety of reasons. Perhaps most important are the ease in fabricating ultrathin, pinhole-free Al_2O_3 layers, spin conservation demonstrated across Al_2O_3 barriers [6], and the first successful demonstrations of the TMR effect using Al_2O_3 barriers [2–4]. Significant efforts have been invested to characterize, understand, and improve properties of alumina barriers (see, e.g., [67–72]). Nevertheless, in the last few years several alternative barriers have been successfully employed, some with very distinct behaviour as compared to Al_2O_3.

Probably the most remarkable result was obtained by de Teresa *et al* [9], who found that the tunnelling spin polarization depends explicitly on the insulating barrier. They used half-metallic LSMO as one of the electrodes with Al_2O_3 or $SrTiO_3$ barriers, or with a composite Al_2O_3/$SrTiO_3$ barrier. Since it is known that LSMO has only majority states at E_F, the tunnelling spin polarization must be positive and close to 100% [55, 61], regardless of the insulating barrier used. As expected, de Teresa *et al* found that Co/Al_2O_3/LSMO MTJs have

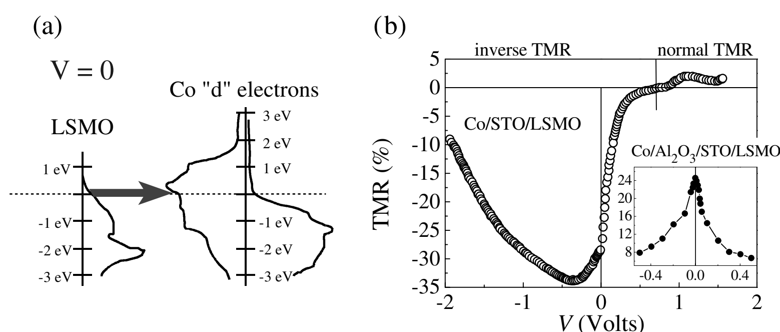

Figure 10. (a) A schematic diagram of the spin-polarized densities of states of LSMO (as derived from photoemission) and the Co(100) surface (calculated). (b) TMR ratio versus applied bias for a Co/$SrTiO_3$/LSMO junction at 5 K. Inverse TMR is observed for $V < 0.8$ V, while normal TMR is observed for $V > 0.8$ V, indicating that the Co/$SrTiO_3$ spin polarization is negative for $V < 0.8$ V. Inset: TMR ratio versus applied bias for a Co/Al_2O_3/$SrTiO_3$/LSMO junction. In this case, the polarizations of Co/Al_2O_3 and LSMO are both positive, and a normal (positive) TMR is seen (from [9]).

a positive TMR for all biases. Surprisingly, however, Co/$SrTiO_3$/LSMO junctions showed *negative* TMR values at zero bias, as shown in figure 10(b). de Teresa *et al* explained these results in terms of the SP of ferromagnet–barrier interfaces rather than the SP of ferromagnets alone. They proposed that the polarization of the Co/$SrTiO_3$ interface must be *negative*—opposite to that of Co/Al_2O_3 interfaces. In order to show this more conclusively, they investigated Co/Al_2O_3/$SrTiO_3$/LSMO junctions, with the expectation that since the LSMO and Co/Al_2O_3 tunnelling SP are both positive, a normal positive TMR would result for all biases. As shown in the inset to figure 10(b), a normal positive TMR is indeed observed for all biases, with a bias dependence that is essentially identical to that of standard Co/Al_2O_3/Co junctions. de Teresa *et al* [9] interpreted the sign change of the Co tunnelling spin polarization in terms of interface bonding, the effect of which was proposed earlier by Tsymbal and Pettifor [73] and will be discussed in section 4.2.

More recent results obtained by Sugiyama *et al* [74] and Sun *et al* [75] essentially corroborated these results. Experiments by Sharma *et al* [39] utilizing Ta_2O_5/Al_2O_3 composite barriers showed that the sign of the spin polarization at Ta_2O_5 interfaces varies with bias voltage and proposed an explanation similar to that of de Teresa *et al* [9]. All these results clearly illustrate the rich physics behind SDT in MTJs, as well as the intriguing possibility of 'engineering' MTJs with tailored properties.

Among other barriers, MgO has been used by a number of researchers. Platt *et al* [76] first demonstrated a large TMR (about 20% at 77 K) in MTJs based on a reactively sputtered MgO barrier. Recently a few successful attempts have been made to grow *epitaxial* MgO barriers. Wulfhekel *et al* [77] and Klaua *et al* [78] fabricated epitaxial Fe/MgO/Fe MTJs on Fe whiskers and extensively investigated the growth and the local transport properties of these junctions. TMR studies of these MTJs were, however, hampered by the difficulties in decoupling the magnetic electrodes from the Fe whisker substrate. Successful magnetotransport experiments on epitaxial Fe/MgO/FeCo(100) MTJs have recently been performed by Bowen *et al* [79] who demonstrated 27% TMR at room temperature, which increased to 60% at 30 K. From the bias dependence of TMR and the theoretical predictions [80], they concluded that s-character electrons are predominantly tunnelling across the 20 Å MgO barrier. Among other barriers, HfO_2 [81] and Ta_2O_5 [76, 82] were successfully used in MTJs.

MRAM and sensor applications of MTJs require, in addition to high values of TMR, a reduced resistance–area (RA) product. Typical values which are required are 100 $\Omega\ \mu m^2$ for MRAMs and less than 0.5 $\Omega\ \mu m^2$ with TMR at least 10% for field sensors. These requirements stimulated research on various oxide barriers. Sharma *et al* [83] have fabricated AlN and AlO_xN_y barriers, observing up to 18% TMR at room temperature with a lower RA product than similar alumina-based junctions as well as a less severe voltage dependence of the TMR. Similarly, Wang *et al* [84] have fabricated junctions with AlO_xN_y with as little as <10% O present, and found TMR values ranging from 13 to 33% and RA products from 73 to 8500 $\Omega\ \mu m^2$, comparable to pure Al_2O_3. Li *et al* [85] have reported similar results with Ga_2O_3. Freitas *et al* have demonstrated MTJs with ZrO_2 [86] or $ZrAlO_x$ [87] barriers, and in both cases the TMR values were comparable to those for similar junctions with Al_2O_3 barriers but with a much reduced RA product. Thus, at the present time, ZrO_2, $ZrAlO_x$, AlN, AlO_xN_y, and Ga_2O_3 barriers can be considered as alternatives to Al_2O_3 for memory and sensor applications of MTJs.

Up to now, we have focused on tunnelling between ferromagnetic electrodes which served as the source of spin polarization. However, the tunnelling spin polarization can be obtained (even with non-magnetic electrodes) due to a SDT probability. The latter may be achieved by utilizing a magnetic tunnel barrier, such as EuS, which is a ferromagnetic semiconductor with $T_C = 16.7$ K [88, 89]. Below T_C the EuS conduction band is exchange split, and tunnelling electrons see a spin-dependent barrier height. For EuS, a typical barrier height is about 2 eV [90], with a conduction band exchange splitting of $\sim$0.36 eV [88, 89]. Given the exponential dependence of tunnel current on barrier height, a highly spin-polarized current is expected.

The principle of spin filtering has been experimentally demonstrated in field emission [89, 91] and in SDT [90] experiments. In the latter case, Moodera *et al* [90] performed SDT experiments using Al/EuS/M junctions, where M was Ag, Au, or Al, and found a tunnelling spin polarization of approximately 80%. Further, using a related Eu chalcogenide, EuSe, Moodera *et al* were able to demonstrate essentially 100% spin polarization. Thus, spin filtering can be considered as an attractive route for the generation and manipulation of highly spin-polarized currents. In particular, combining ferromagnetic electrodes and spin filtering, new hybrid devices and novel effects may be envisaged (see, e.g., [92]).

3.6. Interface dependence

The tunnelling current in MTJs is very much influenced by the electronic structure around the interfaces between the ferromagnetic electrodes and the insulating barrier. One of the ways to explore the interface sensitivity is to insert ultrathin layers (often called ‘dusting’ layers) at the electrode–barrier interfaces. Tedrow and Meservey [93] used the SDT technique to study the spin polarization of ultrathin ferromagnets and showed that only a few monolayers of ferromagnetic material are needed for full tunnelling spin polarization. Moodera *et al* [94] applied this method to measure the spin polarization in $Al/Al_2O_3/Au/Fe$ junctions as a function of Au interlayer thickness. They found that SP decreased exponentially for the first two monolayers of Au, but decreased as $1/d$ at larger thicknesses. In the context of MTJs, Parkin investigated TMR as a function of the thickness of a non-ferromagnetic layer grown on Al_2O_3 [95]. In these experiments, a large tunnelling spin polarization was, surprisingly, maintained over distances in excess of 10 nm, in striking contrast with the earlier experiments of Moodera [94], as well as later experiments by Sun and Freitas for Cu on Al_2O_3 [96].

Recently LeClair *et al* [10] have shown that this apparent discrepancy is related to the growth of MTJs. They grew Cu interlayers both above *and* below the Al_2O_3 barrier, which

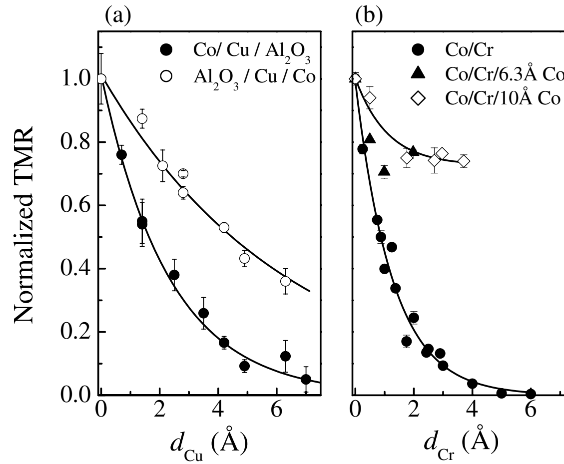

Figure 11. (a) Normalized TMR at 10 K as a function of Cu thickness for Co/Cu(d_{Cu})/Al_2O_3/Co and Co/Al_2O_3/Cu(d_{Cu})/Co. (b) Normalized TMR at 10 K as a function of Cr thickness for Co/Cr(d_{Cr})/Al_2O_3/Co and Co/Cr(d_{Cr})/Co(d_{Co})/Al_2O_3/Co tunnel junctions. Adding only a few monolayers of Co on Cr almost completely restores the TMR, demonstrating the interfacial sensitivity of MTJs. Curves are fits to an exponential decay (from [11, 12]).

resulted in two different TMR decay lengths, as shown in figure 11(a). For Cu above the Al_2O_3 barrier, the length scale was roughly three times larger than for Cu below the Al_2O_3 barrier. They were able to show that Cu grows on Al_2O_3 in a three-dimensional manner, giving rise to an artificially inflated TMR decay. It was further shown that in Co/Cu/Al_2O_3/Co junctions, where Cu was grown on Co rather than on Al_2O_3, near-ideal Cu growth resulted. In this latter system, LeClair *et al* found that the normalized TMR (i.e., $\mathrm{TMR}(d_{\mathrm{Cu}})/\mathrm{TMR}(d_{\mathrm{Cu}} = 0)$) decayed approximately exponentially with increasing Cu thickness, $\exp(-d_{\mathrm{Cu}}/\xi)$. Fitting the TMR decay gave $\xi \sim 0.26$ nm, equivalent to just more than one monolayer of Cu. Appelbaum and Brinkman [97] first pointed out that tunnelling in non-superconducting junctions should be sensitive to the DOS within a few Fermi wavelengths (i.e., $1/k_F$) of the electrode–barrier interface. In this case, ξ is about $3.5k_F^{-1}$, suggesting that k_F^{-1} may indeed be the relevant length scale, at least in disordered systems. This is supported by the results of Moodera *et al* [98] with Ag and Au interlayers, which have almost the same value of k_F^{-1} and give a length scale similar to Cu interlayers, as do Pt interlayers.

A further demonstration of interface sensitivity was subsequently obtained by LeClair *et al* [11], using ultrathin Cr layers in Co/Cr/Al_2O_3/Co MTJs. The TMR decay was again approximately exponential, and in this case was even more rapid (see figure 11(b)) with $\xi \sim 0.1$ nm, or only ~0.5 ML of Cr. In these experiments, they also added an additional Co layer on top of the Cr dusting layer, i.e., Co/Cr(d_{Cr})/Co/Al_2O_3/Co, shown in figure 11(b). Strikingly, the TMR was almost completely restored with only 3–5 ML of Co. This further confirms that just the few monolayers of the electrode adjacent to the ferromagnet–insulator interface dominate MTJ properties, in very good agreement with earlier SDT work on ultrathin magnetic layers.

A theory predicts an oscillatory dependence of TMR on interlayer thickness due to quantum-well states formed in the interlayer [99, 100] (see also section 5.1). Although no quantum-well states were observed in the studies above, in retrospect one would not expect to observe them except in a nearly perfect epitaxial system, as is the case for

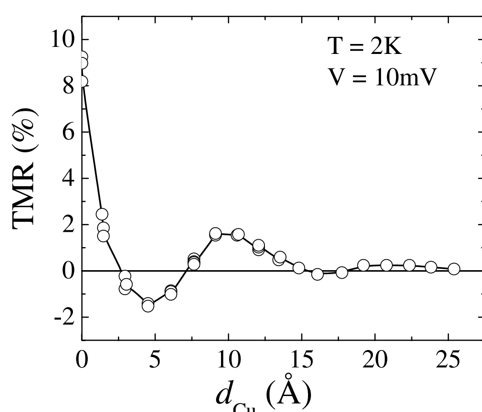

Figure 12. TMR at 2 K and a bias of 10 mV as a function of Cu interlayer thickness for $Co(001)/Cu(001)/Al_2O_3/Ni_{80}Fe_{20}$ junctions. The period of the oscillation observed, 11.4 Å, is in agreement with the Fermi surface of Cu (from [101]).

quantum-well states in metallic multilayers. Yuasa *et al* [101] have recently prepared $Co(001)/Cu(001)/Al_2O_3/Ni_{80}Fe_{20}$ junctions with bottom epitaxial Co/Cu electrodes and observed the true quantum-well oscillations of the TMR that are shown in figure 12. A clear (damped) oscillation of the TMR is evident, with a period of 11.4 Å, in good agreement with the Fermi surface of Cu. Further, independent measurements on similarly grown Co/Cu/Co trilayers gave an oscillation of the interlayer exchange coupling with a period of 11 Å. This clear correlation suggests that the oscillation does indeed arise from spin-dependent reflection at the Co/Cu interface due to the formation of spin-polarized quantum-well states within the Cu interlayer.

3.7. Coulomb blockade effects

One area of research which has recently been the subject of much work both experimentally and theoretically has focused on the interplay between SDT and the Coulomb blockade in ferromagnetic granular films, double junctions, and single-electron transistors. If a small grain of a ferromagnetic material is inserted in the insulating barrier, tunnelling to the grain is strongly influenced by the charging energy. When an electron tunnels into the grain, the electrostatic energy increases by $e^2/2C$, where C is the capacitance of the grain, and, therefore, tunnelling is blocked unless the barrier presented by the charging energy is overcome by bias voltage or thermal energy. The discreteness of the electron charge manifests itself as characteristic Coulomb staircases in the current–voltage characteristics of the junction. Recent theories [102–106] have predicted that the combination of the Coulomb blockade and SDT can lead to both an enhancement and an oscillatory bias dependence of the TMR.

Realizing a system where these effects can be observed is an experimental challenge, however. Granular systems, such as Co clusters in Al_2O_3, are by far the easiest to obtain, and an enhancement of the TMR at low temperatures has been observed [107–110], but the wide distribution of cluster sizes, and hence charging energies, tends to smear out the predicted oscillatory behaviour of the TMR. Recently, however, this problem has been addressed by depositing a granular film in a nanoscale constriction, such that the number of clusters within the measured region is small. By additionally gaining better control over the size distribution of the clusters, the predicted oscillatory behaviour of the TMR has recently been observed in both the CIP [110] and CPP [111] geometries. In the former case, a clear enhancement of the TMR was observed just above the Coulomb blockade threshold voltage, though the oscillation was heavily damped due to relatively large lateral dimensions. In the latter case, however, the CPP geometry afforded much smaller dimensions, and both an enhanced TMR above

the threshold voltage and strong oscillatory behaviour were observed. While the qualitative behaviour of the TMR oscillation with bias voltage is in agreement with theory, most recent theories [102–104, 106] predict that the TMR remains positive for all biases, while the CPP experiments observe a clear sign change of the TMR. One possible origin for the sign change of the TMR is spin accumulation within the clusters, as predicted by Imamura *et al* [105]. In any case, the significantly enhanced and oscillatory TMR in the Coulomb blockade region is a clear verification of the interesting interplay between the Coulomb blockade and SDT, which should stimulate further interest in this growing area of research.

4. Models for perfect junctions

A realistic description of SDT requires taking into account accurate atomic, electronic, and magnetic structure of MTJs. In general, the quantitative description is rather complicated because transport properties depend exponentially on the properties of the barrier, such as the potential barrier height and the barrier thickness, and are very sensitive to the interfacial roughness, impurity states in the barrier, and other types of disorder. In this section we consider perfect tunnel junctions. We ignore, therefore, any type of electron scattering which can affect tunnelling conductance, thereby assuming purely ballistic transport over the whole MTJs. The influence of disorder will be discussed in section 5.

We focus on MTJs which are periodic in the plane parallel to the ferromagnet/barrier interfaces. The assumption of the transverse periodicity of a MTJ simplifies significantly the calculation of transport properties. In this case the electron transverse momentum $\boldsymbol{k}_\parallel$ is conserved, and the tunnelling conductance can be represented as the sum over $\boldsymbol{k}_\parallel$. For the analysis of the conductance it is convenient to use the Landauer–Büttiker formula [112] which, in this case, has the form

$$G = \frac{e^2}{h}\sum_{\boldsymbol{k}_\parallel} T(\boldsymbol{k}_\parallel), \tag{11}$$

where G is the conductance per spin channel, $T(\boldsymbol{k}_\parallel)$ is the transmission coefficient, and the summation is performed over the two-dimensional Brillouin zone. The calculation of the transmission coefficients depends on the particular model which is used for the description of a MTJ. Below we first consider simple free-electron models and then analyse more sophisticated approaches which include a multiband electronic structure of the ferromagnets and the barrier.

4.1. Free-electron models

The simplest insight into TMR can be obtained within a free-electron model by assuming a rectangular potential barrier for tunnelling. Within this model the exchange splitting of the free-electron bands can be included by considering different potentials for the up- and down-spin electrons, $V_\uparrow$ and $V_\downarrow$. For electrons tunnelling between two identical ferromagnetic electrodes across the rectangular barrier of potential U and thickness d, which is assumed to be not too small, the transmission coefficient per spin is given by (e.g., [18, 113])

$$T(k_\parallel) = 16\kappa^2 \frac{k_1}{\kappa^2 + k_1^2}\frac{k_2}{\kappa^2 + k_2^2}\mathrm{e}^{-2\kappa d}, \tag{12}$$

where $k_i = \sqrt{(2m/\hbar^2)(E - V_{\uparrow,\downarrow}) - k_\parallel^2}$ is the spin component of the wavevector normal to the interfaces in the ferromagnets (designated by index $i = 1, 2$) at the Fermi energy E_F, and $\kappa = \sqrt{(2m/\hbar^2)(U - E_F) + k_\parallel^2}$ is the decay constant inside the barrier.

In the limit of a thick barrier only electrons which are characterized by the smallest decay constant κ, i.e. those propagating normal to the interface with $k_{\parallel} = 0$, contribute to the tunnelling current. In this limit the spin polarization of the conductance is given by Slonczewski's formula (10). For barriers that are not too thick the SP depends on the barrier thickness due to the redistribution of tunnelling electrons in the $\boldsymbol{k}_{\parallel}$-space. This fact was shown in model calculations of MacLaren *et al* [113], who illustrated the sensitivity of the TMR ratio to the barrier height and thickness. These calculations demonstrate that even within the simplest free-electron description, the SP and TMR are not determined by characteristics of the ferromagnets alone: they also depend on the properties of the barrier.

Free-electron models were used by a number of researchers to predict magnetoresistive properties of MTJs with paramagnetic layer(s) inserted at the ferromagnet/insulator interface(s) [99, 114, 115]. Vedyayev *et al* [99] found that the conductance and TMR oscillate with the thickness of the inserted layer. These oscillations are the consequence of quantum-well states in the paramagnetic layer resulting in quantum interference of electron waves. They also demonstrated that a large enhancement in the TMR value could be achieved when two paramagnetic layers at the two interfaces have same thickness. The quantum oscillations of TMR with the thickness of a non-magnetic layer were also found by Mathon and Umerski [100], who used realistic tight-binding bands of Co and Cu to calculate the TMR in the presence of a Cu layer inserted at the Co/vacuum interface. Possible enhancements of TMR due to quantum-well states were predicted within free-electron models for double-barrier junctions in which a third ferromagnetic layer is inserted within the barrier [116–118].

In order to observe these quantum effects, the electrons should preserve their coherence in the tunnelling process. Intermixing between transport modes with different transverse momenta $\boldsymbol{k}_{\parallel}$ due to scattering by disorder and impurities could destroy the predicted behaviour. Zhang and Levy [114] proposed that the rapid drop of TMR observed for most MTJs with inserted non-magnetic layers at the interfaces is due to the loss of coherence in transmission through these layers which is caused by fluctuations in the inserted layer thickness. The recent observation of quantum oscillations of TMR in Co/Cu/Al_2O_3/$Ni_{80}Fe_{20}$ tunnel junctions with epitaxial Co/Cu(001) layers by Yuasa *et al* [101] (see also section 3.6) indicates that the quantum coherence can be preserved in real MTJs.

Although free-electron models capture some important features of SDT, they cannot be used for the quantitative description of TMR. In particular, results of the free-electron consideration are very sensitive to the profile of the potential barrier [119]. Moreover, free-electron models ignore the multiband electronic structure of the ferromagnetic electrodes and the ferromagnet/insulator interfaces. Finally, the free-electron models do not take into account the complex band structure of the insulator that, as we will see in section 4.3, is decisive for selecting bands which tunnel most effectively across the barrier. All these arguments demonstrate that merely by using an accurate description of the electronic structure of the entire MTJ it is possible to reach quantitative conclusions about TMR.

4.2. Bonding at the ferromagnet/insulator interface

One of the important properties of MTJs, which affects strongly the SDT, is the chemical bonding at the ferromagnet/insulator interface. The bonding mechanism determines the effectiveness of transmission across the interface which can be different for electrons of different characters. Tsymbal and Pettifor [73] showed that for tunnelling from transition-metal ferromagnets across a thin barrier layer, the spin polarization of the conductance depends strongly on the interfacial bonding between the ferromagnet and the insulator. They found that in case of the ssσ bonding the spin polarization of the conductance is positive, which is

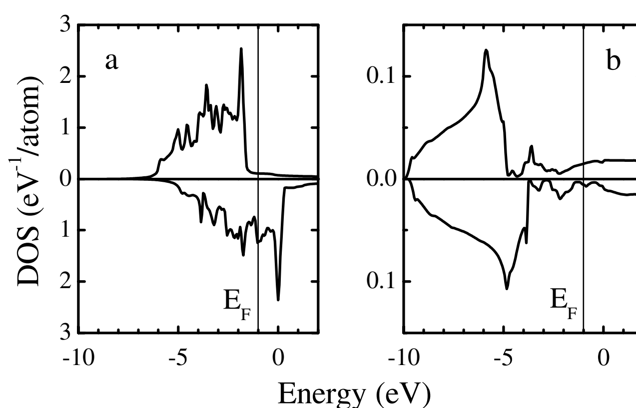

Figure 13. The DOS for bulk fcc Co projected to the d orbitals (a) and the s orbitals (b) for the majority-spin electrons (top panels) and minority-spin electrons (bottom panels). The spin polarization of the d DOS at the Fermi energy is opposite to that for the s DOS. Note the different scales in (a) and (b).

in agreement with experimental data on tunnelling through an alumina spacer [6]. Increasing the sdσ bonding at the interface, however, reduces the spin polarization and can even lead to a change in its sign.

This conclusion can be explained by the fact that in the presence of the interfacial ssσ bonding only s states of the ferromagnet are coupled with those of the insulator. In this case only s electrons of the ferromagnetic layer can contribute to the tunnelling current. It is known, however, that the s component of the DOS is suppressed within the d band of the 3d metals due to the strong s–d hybridization. This is demonstrated in figures 13(a), (b) which show the DOS projected to the d and s orbitals for bulk fcc Co. As is evident from the figure, although the d DOS at the Fermi energy is lower for the majority spins than that for the minority spins, the s DOS is higher, making the spin polarization positive. Increasing the sdσ bonding at the interface, however, results in a large contribution of the d electrons to the tunnelling current. In this case, due to the interfacial sdσ bonding, the d states of the ferromagnet can evolve into the s states of the insulator and can be transmitted across the MTJ. The negative spin polarization of the d DOS at the Fermi energy (see figure 13(a)) can then be reflected in the tunnelling current.

The effect of bonding at the ferromagnet/insulator interface was proposed to explain the experimentally observed inversion of the spin polarization of tunnelling electrons from Co across a $SrTiO_3$ barrier [9] (see section 3.4). The bonding mechanism was also put forward to explain positive and negative values of TMR depending on the applied voltage in MTJs with Ta_2O_5 and Ta_2O_5/Al_2O_3 barriers [39] and to elucidate the inversion of TMR observed in Co-contacted multiwalled carbon nanotubes [120]. Itoh and Inoue predicted theoretically the strong sensitivity of the magnitude of TMR to the sp–d mixing at the ferromagnet/alumina interface in the presence of imperfectly oxidized Al or O ions [121]. Tsymbal *et al* [122] found that oxygen deposited on the surface of Fe inverts the spin polarization of the DOS at the Fermi energy propagating in vacuum, due to hybridization of the iron 3d orbitals with the oxygen 2p orbitals and the strong exchange splitting of the antibonding oxygen states. Earlier *ab initio* calculations of the electronic structure of a Co/HfO_2 tunnel junction [123] demonstrated the inversion of the spin polarization at the Fermi energy. For $Co/SrTiO_3/Co$ tunnel junctions, Oleinik *et al* [124] predicted that the exchange coupling between the interface Co and Ti atoms mediated by oxygen induces a magnetic moment of 0.2 μ_B on the interface Ti

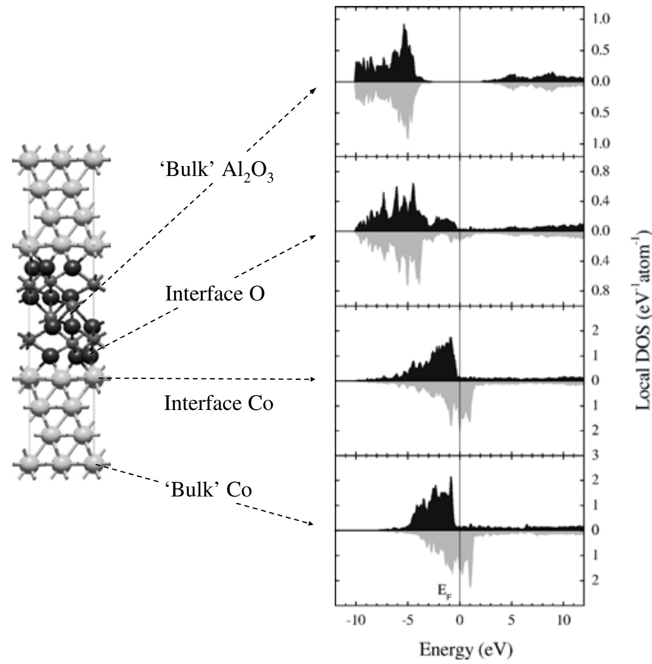

Figure 14. The calculated atomic structure and local DOS for majority-spin electrons (top panels) and minority-spin electrons (bottom panels) for a Co/Al_2O_3/Co tunnel junction (after [125]).

atom, which is aligned antiparallel to the magnetic moment of the Co layer. All these findings indicate an important role of the bonding at the ferromagnet/insulator interface in SDT.

However, despite the importance of the interfacial bonding, this bonding alone is *not* able to explain the positive SP of electrons tunnelling from 3d ferromagnets across an alumina barrier observed experimentally. First-principles calculations of the electronic structure of a Co/Al_2O_3/Co tunnel junction [125] demonstrate the presence of a strong covalent bonding between d orbitals of Co and p orbitals of O at the Co/Al_2O_3 interface. This can be seen from figure 14 which shows the local densities of states corresponding to different atoms in the Co/Al_2O_3/Co tunnel junction. As is evident from the local DOS for the interfacial O atom, the hybridization of the Co 3d states and O 2p states leads to formation of the bonding and antibonding states. The oxygen antibonding states are exchange-split mirroring the strong exchange splitting of the Co 3d states. Although the calculations find a negative spin polarization in the local DOS at the Fermi energy on the O and Al atoms close to the interface (which reflect the negative spin polarization of the DOS in Co), the spin polarization of the DOS becomes positive on interior atoms of the alumina layer [125]. This indicates that the spin polarization of the tunnelling current should also be positive, which is in agreement with the experiments on SDT. In order to explain this behaviour, one needs to consider explicitly the mechanism of conductance in MTJs and identify those bands dominating the tunnelling process. This will be the subject of our discussion in section 4.3.

4.3. First-principles calculations of TMR

First-principles methods based on density functional theory within the local spin density approximation (LSDA) for the electronic structure and the Landauer–Büttiker formula (11) for the conductance provide the basis for an accurate calculation of SDT in MTJs. This approach

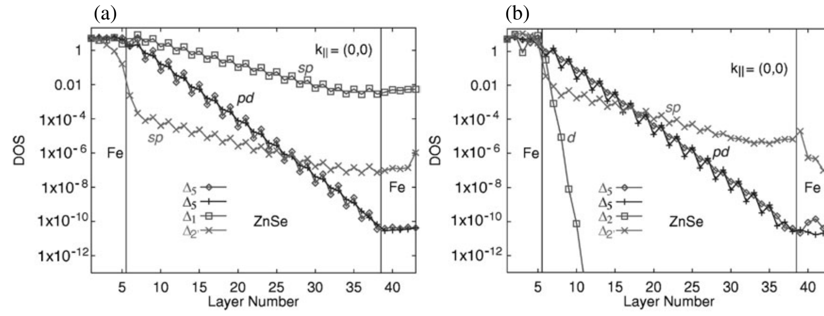

Figure 15. The calculated layer-dependent DOS for the majority (a) and minority (b) Bloch states at $\boldsymbol{k}_{\parallel} = 0$ for the Fe/ZnSe/Fe junction. Different decay rates and injection efficiencies for the states of different characters and symmetries are seen (after [126]).

is advantageous due to a realistic, multiband description of the electronic structure, which takes into account the character and the spin polarization of the electronic states in ferromagnetic electrodes, the interfacial localized states, the variation of the potential across the barrier, and the evanescent states in the insulator.

Using the layered Korringa–Kohn–Rostoker (LKKR) method, MacLaren *et al* [126] calculated the electronic structure and the tunnelling conductance in Fe/ZnSe/Fe(100) MTJs. They found that the spin asymmetry in the conductance increases dramatically with increasing barrier thickness. They showed that the difference in the decay rates for the majority-and minority-spin channels follows from the symmetry of the Bloch states at the Fermi energy, which have different spin injection (extraction) efficiencies and different decay rates when tunnelling across the barrier. Since at a relatively large barrier thickness the conductance is dominated by states at $\boldsymbol{k}_{\parallel} = 0$, they analysed the results in terms of the layer-resolved DOS within the electrodes and the tunnelling barrier at $\boldsymbol{k}_{\parallel} = 0$, as shown in figures 15(a) and (b). As is evident from these figures, there are three decay rates, which are associated with the angular momentum character of the bands within the barrier. The rate of the decay is slowest for bands with s character and most rapid for bands with only d character. In addition to the different decay rates, the ease of injection and extraction depends upon the character of the band in the electrode. For example, in the majority channel, the Δ_1 band, because it is compatible with the s character, couples efficiently with a decaying sp state in the ZnSe, and, thus, this band dominates the conductance. The much smaller tunnelling conductance seen for the minority spins in figure 15(b) is a direct result of there being no Δ_1 band present at the Fermi energy.

On the basis of these results, MacLaren *et al* [126] concluded that the expected spin dependence of the tunnelling current can be deduced from the symmetry of the Bloch states at the Fermi energy. The bands with s character are able to couple most efficiently across the interface, and decay most slowly in the barrier. For Fe, Co, and Ni ferromagnets the majority states at the Fermi energy have more s character than the minority states, which tend to have mainly d character. Thus, the majority conductance is expected to be greater than the minority conductance, resulting in a slower decay with the barrier thickness for the former. These conclusions are expected to be also valid for MTJs with an Al_2O_3 barrier, which is consistent with the experimental observations [6]. This explains an earlier hypothesis of Stearns [7] who proposed that the most dispersive bands are decisive for the tunnelling process.

MacLaren *et al* [126] pointed out that the spin asymmetry in the tunnelling conductance should depend on the substrate crystal face. In the case of Fe, e.g., an examination of the band structure shows that for [100], [111], and [110] directions all have majority bands with

s character present, and for all but the [100] direction, a band with this symmetry also crosses the Fermi energy for the minority channel. Thus, the [100] direction should exhibit the largest asymmetry in the tunnel conductance. Indeed, the dependence of the TMR on the crystal face of the epitaxial Fe electrodes in Fe/Al_2O_3/CoFe junctions was recently observed by Yuasa *et al* [65] (see section 3.4). However, they found larger values of TMR for tunnelling from Fe(110), rather than from Fe(100) electrodes. Still, further analysis of bands contributing to the tunnelling is needed to obtain consistency between the theory and experiment.

Mavropoulos *et al* [127] emphasized the importance of the evanescent gap states in the tunnelling barrier for SDT. They used a notion of the complex band structure to analyse the metal-induced gap states with specific examples of Si, Ge, GaAs, and ZnSe. Using the empirical pseudopotential method, Mavropoulos *et al* calculated the complex band structure of these semiconductors, which enabled them to determine the decay rate parameter $\kappa(\boldsymbol{k}_\parallel, E)$ and the symmetry of the evanescent states. They found that the states which belong to the identity representation Δ_1 should have minimum decay rates for a broad class of materials. For semiconductors (insulators) with a direct band gap (such as GaAs, ZnSe, and semiconductors with a higher atomic number or/and ionicity) these states are centred on the Γ point ($\boldsymbol{k}_\parallel = 0$). However, for indirect band gap semiconductors (such as Si and Ge) these states might be centred on other points in the Brillouin zone depending on the position of the Fermi level with respect to the bottom of the conduction band. Thus, it was demonstrated that the complex band structure of the barrier material allows one to explain very important features of the tunnelling process and can be regarded as one of the fundamental characteristics of spin-dependent conductance in MTJs.

The conclusions drawn from considering the complex band structure are also applicable to oxide barrier MgO [127]. Recently Butler *et al* [80] calculated the electronic structure and the tunnelling conductance in Fe/MgO/Fe MTJs within the approach of their previous work [126]. Their conclusions essentially support findings reported in [126] and [127]. In particular, they found that due to the absence of the minority Δ_1 band at the Fermi energy of Fe(100), the majority-spin conductance dominates tunnelling which leads to a very high TMR for thick enough barriers. Mathon and Umerski [128] arrived at the same qualitative conclusions, after calculating the TMR in Fe/MgO/Fe MTJs using the multiband tight-binding description for the electronic structure. Although not as accurate as first-principles-based theory, this approach is far more realistic than free-electron models, as demonstrated in the modelling of GMR [17]. Earlier, the tight-binding method was used by Mathon [129], who attempted to unify the description for the CPP GMR and TMR phenomena.

In concluding this section, we note that the experiments performed on epitaxial Fe/MgO/FeCo MTJs [79] (see also section 3.5) show much smaller values of TMR compared to those predicted theoretically. This might be due to the formation of a partially oxidized FeO layer at the interface which was found in the experiments by Meyerheim *et al* [130]. In addition, effects of disorder which are ignored in the theoretical studies of [80, 129] may play a significant role. Epitaxial Fe/ZnSe/FeCo MTJs show less impressive behaviour, demonstrating a sizable magnetoresistance of 16% only at low temperatures [131]. This is obviously the consequence of a semiconducting nature of the ZnSe barrier which makes the mechanism of conductance different from that considered theoretically. The presence of impurity/defect states in the electrodes and in the barrier makes the ballistic approach inadequate for the description of SDT in these junctions. The effects of disorder will be discussed in the next section.

5. Models for disordered junctions

Actual tunnel junctions contain large amounts of disorder in the electrodes, in the barrier, and at the electrode/barrier interfaces. This disorder may represent interdiffusion at the interfaces,

interface roughness, impurities, and defects such as grain boundaries, stacking faults, and vacancies. Interdiffusion dramatically changes the electronic and atomic structure, which affects TMR in a critical way (e.g., [132–134]). Interface roughness leads to fluctuations in the barrier thickness that strongly alter the tunnelling conductance [135]. Impurities and defects in the barrier introduce complex mechanisms that assist tunnelling [36, 42, 136–140]. This is especially important in the case of amorphous barriers, although even in epitaxially grown tunnel junctions the effects of disorder might be decisive. Disorder in the electrodes mixes bulk and interface states and thereby influences TMR [141–143]. In this section we consider some consequences of disorder in MTJs that are important for the understanding of experiments on SDT.

5.1. Contribution of interface states

As we saw, for perfect tunnel junctions it is important to identify the propagating (bulk) states in the ferromagnets which are coupled to the slowest-decaying state in the barrier, and therefore dominate tunnelling. However, as was pointed out by Levy *et al* [141], calculations made for purely ballistic transport over the whole junction cannot be directly compared to data on real junctions, because the ballistic conductance underestimates a contribution from states localized near the interfaces. In disordered tunnel junctions these interface states are coupled to the propagating states in the electrodes by diffusive and relaxation processes, which provide additional conduction channels. Under these conditions the electronic structure at the electrode/barrier interfaces may control the tunnelling current.

Although the interface states can contribute to the tunnelling conductance even in perfect MTJs, their contribution is normally small. The interface states from both sides of the barrier are coupled to the propagating states from the other side of the barrier and are coupled to each other. This leads to a resonant mechanism of tunnelling which manifests itself as spikes in the conductance distribution at particular $\boldsymbol{k}_{\parallel}$-points in the two-dimensional Brillouin zone [144]. The width of these spikes is determined by the strength of the coupling through the barrier, which decreases exponentially with the barrier thickness.

The presence of defect scattering in the electrodes and at the electrode/barrier interfaces makes the coupling between the interface and bulk states much more efficient. This affects the spin polarization of tunnelling electrons due to difference in SP of the bulk and interface states. Figure 16 shows a model tight-binding calculation of the conductance across a disordered Fe/I/Fe tunnel junction, in which the insulator (I) is described by a simple tight-binding band that provides no states at the Fermi energy. Disorder is introduced by random variations in the on-site atomic energies of width γ within 10 ML of the Fe electrode adjacent to the interface. As is evident from the figure, in the absence of disorder ($\gamma = 0$) the spin polarization is large, about 0.9. This high value of the spin polarization is consistent with calculations of Butler *et al* [80] and Mathon and Umerski [128] for Fe/MgO/Fe MTJs and reflects the presence of the Δ_1 symmetry band at the Fermi energy for the majority-spin electrons of Fe(100) and the absence of such a band for the minority-spin electrons. With increasing disorder the conductance of the minority spins increases dramatically, whereas the conductance of the majority spins is insensitive to disorder, which leads to a decrease in the spin polarization. The enhancement in the transmission for the minority-spin electrons with disorder is due to the interface states which have a strong weight at the Fermi energy in Fe (see, e.g., [142]). These interface states get coupled to the bulk states within the same electrode and thereby contribute to the conductance. We note that, in addition, disorder breaks the symmetry of the system and mixes the propagating Bloch states in the leads. This makes it possible for the states which are not able to tunnel effectively through the barrier in the perfect tunnel junction by symmetry to be mixed with the states which are and therefore to be involved in transport.

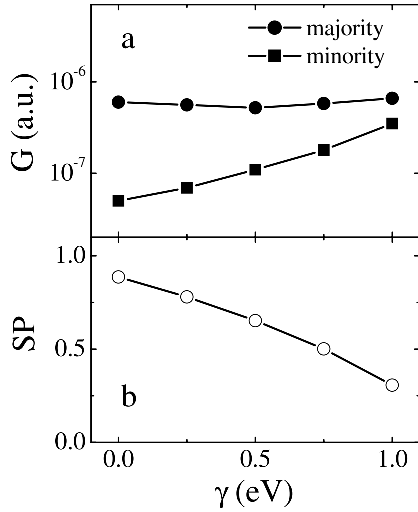

Figure 16. The calculated conductance for the majority- and minority-spin electrons (a) and the spin polarization (b) of the conductance in an Fe/I/Fe tunnel junction as a function of disorder parameter γ. With increasing disorder the SP decreases due to the contribution from the interface state in Fe. A typical value of γ for sputtered 3d-metal films is about 0.5 eV (after [145]).

We see, therefore, that disorder makes the electronic structure at the electrode/barrier interfaces control the tunnelling current. Disorder leads to diffuse scattering that couples the propagating states in the bulk of the electrodes to the states localized at the interfaces. This mechanism is the fundamental origin of the decisive role of the interface electronic structure, which was demonstrated experimentally by LeClair *et al* [10–12] (see section 3.6).

5.2. Effect of disorder in the barrier

Disorder in the barrier layer has a dramatic effect on SDT. The presence of disorder broadens the conduction and the valence bands of the insulator and creates localized electronic states within the band gap. The broadening of the bands reduces the effective potential barrier for tunnelling that, according to Slonczewski [18] (section 2.4), negatively influences the spin polarization of tunnelling electrons in MTJs.

Even more decisive effects occur due to the formation of localized impurity/defect states in the barrier. If the energy of these states is close to the Fermi energy, they lead to resonance tunnelling. In order to understand the consequences of resonant tunnelling in MTJs we consider a simple one-dimensional model for impurity-assisted tunnelling. In this case the conductance per spin is given by

$$G = \frac{4e^2}{h}\frac{\Gamma_1\Gamma_2}{(E_F - E_r)^2 + (\Gamma_1 + \Gamma_2)^2}, \tag{13}$$

where E_F is the Fermi energy, E_r is the energy of the resonant state, and Γ_1 and Γ_2 are rates of leakage of electrons from the impurity state to the left and right electrodes. We assume for simplicity that the latter are proportional to the densities of states of the electrodes, ρ_1 and ρ_2, at the left and right interfaces, so $\Gamma_1 \propto \rho_1 \exp[-2\kappa x]$ and $\Gamma_2 \propto \rho_2 \exp[-2\kappa(d - x)]$, where κ is the decay constant and x is the position of the impurity within the barrier of thickness[6] d. Off resonance, when $|E - E_r| \gg \Gamma_1 + \Gamma_2$, the latter assumption implies that the spin conductance is given by $G \propto \rho_1\rho_2$. When tunnelling occurs between ferromagnetic electrodes this leads to TMR, which is given by Julliere's formula (7), with P_i $(i = 1, 2)$ given by equation (8).

[6] This assumption is valid, e.g., for tunnelling across a relatively high rectangular potential barrier for which $\kappa \gg k_1, k_2$, where k_1 and k_2 are the absolute values of the momenta of electrons in the left and right electrodes respectively.

In order to take into account disorder in real tunnel junctions, the conductance should be averaged over the energies and positions of impurities. Following [136], we assume for simplicity a homogeneous distribution of impurities with uniform density $D(E_r) = \delta$. Integrating equation (13) with respect to the impurity position and energy we obtain for non-half-metallic electrodes ($\rho_i^{\uparrow\downarrow} \neq 0$) and for barriers that are not too thin ($\exp[-\kappa d] = 1$) that

$$\langle G \rangle = \frac{e^2}{h} \frac{\delta \mathrm{e}^{-\kappa d}}{2\kappa d} \sqrt{\rho_1 \rho_2}. \tag{14}$$

For ferromagnetic electrodes this implies that the respective spin polarization of the tunnelling conductance across a disordered barrier is reduced compared to that for a perfect barrier, so

$$P_i = \frac{\sqrt{\rho_i^{\uparrow}} - \sqrt{\rho_i^{\downarrow}}}{\sqrt{\rho_i^{\uparrow}} + \sqrt{\rho_i^{\downarrow}}}, \tag{15}$$

where $i = 1, 2$. This leads to a diminished value of TMR, which is still given by Julliere's formula (7), but the effective SP of the electrodes are defined by equation (15). For example for $\rho^{\uparrow\downarrow} = \rho_1^{\uparrow\downarrow} = \rho_2^{\uparrow\downarrow}$ and $\rho^{\uparrow}/\rho^{\downarrow} = 3$, we obtain $P = 50\%$ and TMR = 67% for a perfect junction, whereas we obtain $P = 27\%$ and TMR = 15% for a disordered junction. This significant reduction in the SP and TMR is the consequence of spin-dependent leak rates, Γ_1 and Γ_2, and the inversion of magnetoresistance at resonant conditions, as we will see in section 5.3.

In real MTJs with amorphous barriers the situation is more complicated because of the contribution from multiple resonances resulting from the interference of electrons scattered by several localized stated in the barrier. Tsymbal and Pettifor [138] found that in strongly disordered tunnel junctions the tunnelling current flows through a few regions of the insulator where local disorder configuration provides highly conducting channels for electron transport. This mechanism of conduction leads to a broad distribution of the tunnelling current, which is in agreement with experimental data on local transport properties of Al_2O_3 tunnel barriers [135]. Tsymbal and Pettifor predicted a decrease in the spin polarization of the tunnelling current with disorder and insulator thickness. Interestingly, they found that the TMR is in agreement with Julliere's formula (7), in which $P_{1,2}$ is defined as the spin polarization of the tunnelling current from the ferromagnet to a non-magnetic metal. This might explain the success of the Julliere's formula when comparing the TMR magnitudes with the SP values measured in experiments on superconductors (section 3.4).

Several authors addressed the problem of the influence of magnetic impurities within the barrier on TMR [42, 139, 140]. In particular, Vedyayev *et al* [42] found that at low temperatures and zero bias voltage, the TMR in a MTJ with paramagnetic impurities can be larger than that of the same structure without paramagnetic impurities. They also found that an increase in temperature leads to a decrease in the TMR magnitude due to the excitation of spin-flip processes resulting in mixing of spin-up and spin-down channels. Jansen and Lodder [139] showed that for spin-polarized states in the barrier, the magnetoresistance due to resonant tunnelling can be enhanced compared to the magnetoresistance due to direct tunnelling. Inoue *et al* [140] extended the treatment of the tunnel conductance to take into account many-body effects of the exchange interaction between the tunnelling electrons and localized spins. They found that the TMR ratio decreases by approximately 10% due to the spin-flip process caused by the exchange interaction.

5.3. TMR at resonant conditions

Equation (13) for resonant tunnelling predicts a strong variation of TMR as a function of the impurity energy near the resonance (similar to that shown in figure 17(c)). Exactly at the resonance, i.e. when $E_F - E_r = 0$, the magnetoresistance is inverted. Indeed, assuming for simplicity an asymmetric position of the impurity we obtain from equation (13) that $G \propto \rho_2/\rho_1$ if $x < d/2$ and hence $\Gamma_1 = \Gamma_2$, and we obtain that $G \propto \rho_1/\rho_2$ if $x > d/2$ and hence $\Gamma_1 = \Gamma_2$. In both cases, the conductance is inversely proportional to the DOS of the one of the ferromagnets which results in the sign inversion of the TMR:

$$\mathrm{TMR} = -\frac{2P_1P_2}{1+P_1P_2} \tag{16}$$

(compare to equation (7)). As we see, the inversion of the TMR originates from the spin-dependent leak rates that under resonant conditions invert the effective SP of that of the ferromagnetic electrodes.

The question arises of whether it is possible to observe the strong variation and the inversion of magnetoresistance at resonant conditions. As we saw in the previous section, the averaging over a large number of disorder configurations corresponding to different energies and positions of impurities simply results in the suppression of TMR. This is due to a relatively large area of thin-film tunnel junctions, which normally spans values from a fraction of a $\mu\mathrm{m}^2$ to a few mm^2. Very recently, Tsymbal *et al* [146] found that it is possible to reveal effects dominated by a single localized state and to observe a broad distribution of TMR values including the inverse magnetoresistance in magnetic nanojunctions with a small cross-section. As was demonstrated earlier by Doudin *et al* [147], nanowire junctions grown by electrodeposition with a cross-section less than 0.01 $\mu\mathrm{m}^2$ display two-level fluctuations of the electric current which indicate an impurity/defect-driven transport. By performing measurements on a large number of samples and comparing experimental and calculated statistics, Tsymbal *et al* [146] showed that the TMR is inverted when the energy of a localized state in the barrier matches the Fermi energy of the ferromagnetic electrodes. The experimental and calculated distributions of the TMR along with the predicted energy dependence of the magnetoresistance for a tunnel junction demonstrating the inverse TMR are displayed in figure 17.

Another possible way to observe the predicted strong variation of TMR due to resonant tunnelling is to use local characterization techniques such as STM [77] and BEEM [148]. As was shown by Tsymbal and Pettifor [149], in this case a local impurity/defect state in the barrier can be detected due to electrons ballistically traversing the top metallic layer and, then, tunnelling resonantly across the barrier via the localized electronic state in the band gap of the insulator. They found that the TMR magnitude varies dramatically as the tip scans the area above the impurity atom. If the tip is located directly above the impurity, the TMR is inverted. This phenomenon could be observed by the STM or BEEM techniques provided that the switching of the magnetic alignment of the two electrodes in a MTJ is achieved. Note that the BEEM technique [148] has the advantage of the intrinsic ballistic nature of the transit current, whereas the STM technique [77] requires the use of high-quality epitaxial junctions.

6. Conclusions

Stimulated by the discovery of GMR in metallic magnetic multilayers (for a recent review on GMR see [17]), spin electronics has developed into a vigorous field of research. SDT in MTJs, one of the areas of spin electronics, has aroused considerable interest due to a large room temperature magnetoresistance. Significant progress in the fabrication and characterization of MTJs and in the understanding of basic mechanisms which control the spin polarization

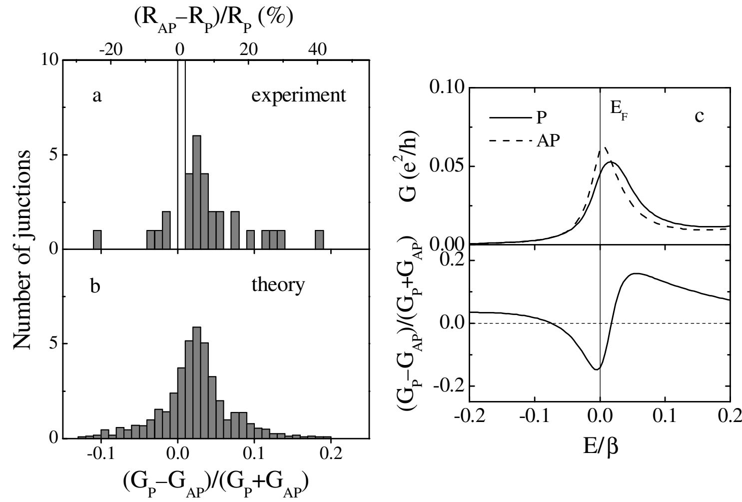

Figure 17. Experimental (a) and calculated (b) distributions of the magnetoresistance in magnetic Ni/NiO/Co nanojunctions and (c) the predicted conductance for parallel ('P') and antiparallel ('AP') configurations of the electrodes (top) and TMR as a function of energy for a tunnel junction which shows the inverse TMR (bottom). The highest positive and negative values of magnetoresistance measured are +40% and −25%. The unshaded bar indicates a possible contribution from samples with multiple junctions (after *et al* [146]).

of tunnelling electrons have been achieved in the past few years. This has led to important advances towards applications of magnetoresistive devices based on MTJs, such as random-access memories (e.g., [26, 150]), as well as elucidating the fundamental physics that governs the functioning of these devices.

One of the breakthroughs in the understanding of TMR is the recognition of the fact that the tunnelling spin polarization in MTJs is not only determined by the properties of the ferromagnets but also depends on the atomic and electronic structure of the entire junction including the insulator and the ferromagnet/insulator interfaces. This broadens dramatically the possibilities for altering the properties of MTJs. In particular, by modifying the electronic properties of the tunnelling barrier and the ferromagnet/insulator interfaces it is possible to engineer MTJs with properties desirable for device applications.

There has been a significant progress in the theoretical description of TMR. First-principles calculations of the electronic structure and the conductance in MTJs have led to deeper insights into the role of symmetry of the electronic states of the ferromagnets and their coupling to the evanescent states in the barrier. These calculations have also demonstrated the importance of the interfacial states and the character of chemical bonding across the metal/insulator interfaces. More can be expected from *ab initio* models in addressing the role of defects at the interfaces such as the partially oxidized Fe layer in Fe/MgO/Fe epitaxial junctions [130]. In general, including defect scattering is an important ingredient for further progress in the theoretical description of TMR. However, a proper first-principles treatment of all the existing defects might be too expensive computationally and, therefore, reliable simplified models become of great importance.

The voltage dependence of TMR is far from being completely understood. The difficulty arises from the fact that a number of different processes may contribute to the voltage dependence, such as the spin-dependent electronic structure of the electrodes, inelastic scattering by defect/impurity states in the barrier, and electron–phonon, electron–magnon, and

electron–electron interactions. For a realistic theoretical description of the voltage dependence, it might be necessary to incorporate the non-equilibrium Green function formalism into the theory of TMR [151]. Further studies have to be performed to elucidate the role of different mechanisms in the voltage dependence.

There is unrealized potential of half-metallic-based tunnel junctions. Ideally incorporation of 100% spin-polarized ferromagnets into a MTJ should lead to an infinitely large TMR. Unfortunately, experiments so far show an unimpressive behaviour of MTJs based on half-metals at room temperature. A possible reason for this is the poor quality of the half-metal/barrier interfaces, resulting in a dramatic reduction of the spin polarization and/or a detrimental effect of thermal fluctuations on the spin polarization [152]. More work has to be done to obtain well-controlled half-metallic films and interfaces with robust spin polarization.

The success of SDT in MTJs has exposed a number of new directions for further research. In particular, spin-electronics applications based on magnetotransport phenomena in semiconductors have recently started to attract more and more attention. Making use of semiconductors in spin electronics has the advantage of incorporating the magnetoresistive devices into existing semiconductor technologies. The feasibility of using semiconductors is supported by their capability of carrying highly spin-polarized currents over long distances [153] and by the successful demonstration of electrical spin injection from magnetic dilute semiconductors [154, 155]. Recent discoveries of room temperature spin injection from metallic Fe into GaAs [156, 157], a large magnetoresistance in GaMnAs/AlAs tunnel junctions [158], and the possibility of spin filtering across ferromagnet/semiconductor interfaces at room temperature [159] stimulated further interest in this field. The advances in the understanding of mechanisms controlling quantum magnetotransport in MTJs are expected to be very much instrumental in achieving progress in this very rapidly developing area of spin electronics.

Another example is the ballistic conductance in magnetic nanocontacts. Experiments performed on nanocontacts fabricated from Ni nanowires have shown sizable values of magnetoresistance at room temperature [160]. These experiments have been explained by the domain wall constrained by the nanocontact region [161, 162]. Very recent studies on electrodeposited Ni nanocontacts found, however, that it is possible to achieve magnetoresistance as high as 3000% at room temperature [163], which can hardly be explained by just spin-dependent scattering by the constrained domain wall. The physical mechanism causing this phenomenon is, at present, unknown and further studies, both theoretical and experimental, are desirable.

Elucidating spin-dependent conductance in metallic nanocontacts is also important for the understanding of the electronic transport through pinholes in MTJs. As was discovered recently [164], in some cases pinholes in a tunnel barrier may mimic tunnelling and make it difficult to distinguish between electron conduction through pinholes and direct tunnelling. Recent experiments showed that it is possible to observe 15% magnetoresistance at room temperature from electrodeposited nanocontacts through pinholes in MTJs [165].

Using spin-polarized barriers in MTJs may be promising for applications as spin filters. The demonstration of highly efficient spin-filter tunnelling using EuS [92] should stimulate further research in this field—in particular, in the search for spin-polarized barriers which preserve their properties at room temperature. Next-generation devices based on spin-filter tunnel structures have potential for highly efficient spin injection into semiconductors [166], essential for the development of semiconductor-based spin electronics.

In summary, SDT in MTJs is a fast-growing area of research, which combines both tremendous technological potential and deep fundamental physics. It has stimulated new directions in spin-dependent electronic transport, which promise exciting results in the future.

Acknowledgments

EYT acknowledges funding from the National Science Foundation (DMR-0203359 and MRSEC: DMR-0213808) and the Nebraska Research Initiative. A collaborative research programme of the University of Nebraska-Lincoln and Seagate Research is gratefully acknowledged as an important factor stimulating the work on this review article.

References

[1] Julliere M 1975 *Phys. Lett.* A **54** 225
[2] Miyazaki T and Tezuka N J 1995 *J. Magn. Magn. Mater.* **139** L231
[3] Moodera J S, Kinder L R, Wong T M and Meservey R 1995 *Phys. Rev. Lett.* **74** 3273
[4] Parkin S S P, Roche K P, Samant M G, Rice P M, Beyers R B, Scheuerlein R E, O'Sullivan E J, Brown S L, Bucchigano J, Abraham D W, Lu Yu, Rooks M, Trouilloud P L, Wanner R A and Gallagher W J 1999 *J. Appl. Phys.* **85** 5828
[5] Tedrow P M, Meservey R and Fulde P 1970 *Phys. Rev. Lett.* **25** 1270
Tedrow P M and Meservey R 1971 *Phys. Rev. Lett.* **26** 192
Tedrow P M and Meservey R 1973 *Phys. Rev.* B **7** 318
[6] Meservey R and Tedrow P M 1994 *Phys. Rep.* **238** 173
[7] Stearns M B 1977 *J. Magn. Magn. Mater.* **5** 1062
[8] Moodera J S, Nassar J and Mathon G 1999 *Annu. Rev. Mater. Sci.* **29** 381
[9] de Teresa J M, Barthelemy A, Fert A, Contour J P, Lyonnet R, Montaigne F, Seneor P and Vaurès A 1999 *Phys. Rev. Lett.* **82** 4288
de Teresa J M, Barthelemy A, Fert A, Contour J P, Lyonnet R, Montaigne F, Seneor P and Vaurès A 1999 *Science* **286** 507
[10] LeClair P, Swagten H J M, Kohlhepp J T, van de Veerdonk R J M and de Jonge W J M 2000 *Phys. Rev. Lett.* **84** 2933
[11] LeClair P, Kohlhepp J T, Swagten H J M and de Jonge W J M 2001 *Phys. Rev. Lett.* **86** 1066
[12] LeClair P, Hoex B, Wieldraaijer H, Kohlhepp J T, Swagten H J M and de Jonge W J M 2001 *Phys. Rev.* B **64** 100406
[13] Levy P M and Zhang S 1999 *Curr. Opin. Solid State Mater. Sci.* **4** 223
[14] Monsma D J and Parkin S S P 2000 *Appl. Phys. Lett.* **77** 720
[15] Soulen R J, Byers J M, Osofsky M S, Nadgorny B, Ambrose T, Cheng S F, Broussard P R, Tanaka C T, Nowak J, Moodera J S, Barry A and Coey J M D 1998 *Science* **282** 85
Mazin I I 1999 *Phys. Rev. Lett.* **83** 1427
[16] Maekawa S and Gäfvert U 1982 *IEEE Trans. Magn.* **18** 707
[17] Tsymbal E Y and Pettifor D G 2001 *Solid State Physics* vol 56, ed H Ehrenreich and F Spaepen (New York: Academic) pp 113–237
[18] Slonczewski J C 1989 *Phys. Rev.* B **39** 6995
[19] Suezawa Y, Takahashi F and Gondo Y 1992 *Japan. J. Appl. Phys.* **31** L1415
[20] Nowak J and Rauluszkiewicz J 1992 *J. Magn. Magn. Mater.* **109** 79
[21] Yaoi T, Ishio S and Miyazaki T 1993 *J. Magn. Magn. Mater.* **126** 430
[22] Plaskett T S, Freitas P P, Barradas N P, da Silva M F and Soares J C 1994 *J. Appl. Phys.* **76** 6104
[23] LeClair P, Moodera J S and Meservey R 1994 *J. Appl. Phys.* **76** 6546
[24] For a review on exchange biasing see
Nogues J and Schuller I K 1999 *J. Magn. Magn. Mater.* **192** 203
Berkowitz A E and Takano K 1999 *J. Magn. Magn. Mater.* **200** 552
[25] Gider S, Runge B U, Marley A C and Parkin S S P 1999 *Science* **281** 797
[26] Tehrani S, Engel B, Slaughter J M, Chen E, De Herrera M, Durlam M, Naji P, Whig R, Janesky J and Calder J 2000 *IEEE Trans. Magn.* **36** 2752
[27] LeClair P 2002 *PhD Thesis* Eindhoven University of Technology
[28] Moodera J S and Kinder L R 1996 *J. Appl. Phys.* **79** 4724
[29] Yuasa S, Sato T, Tamura E, Suzuki Y, Yamamori H, Ando K and Katayama T 2000 *Europhys. Lett.* **52** 344
[30] Boeve H, Girgis E, Schelten J, De Boeck J and Borghs G 2000 *Appl. Phys. Lett.* **76** 1048
[31] Zhang S, Levy P M, Marley A and Parkin S S P 1997 *Phys. Rev. Lett.* **79** 3744
[32] Han X-F, Yu A C C, Oogane M, Murai J, Daibou T and Miyazaki T 2001 *Phys. Rev.* B **63** 224404
[33] Moodera J S, Nowak J and van de Veerdonk R J M 1998 *Phys. Rev. Lett.* **80** 2941

[34] Wulfhekel W, Ding H F and Kirschner J 2002 *J. Magn. Magn. Mater.* **242–245** 47
[35] Zhang J and White R 1998 *J. Appl. Phys.* **83** 6512
[36] Jansen R and Moodera J S 1998 *J. Appl. Phys.* **83** 8882
Jansen R and Moodera J S 2000 *Phys. Rev.* B **61** 9047
[37] Jansen R and Moodera J S 1999 *Appl. Phys. Lett.* **75** 400
[38] LeClair P, Kohlhepp J T, van de Vin C H, Wieldraaijer H, Swagten H J M and de Jonge W J M 2002 *Phys. Rev. Lett.* **88** 107201
[39] Sharma M, Wang S X and Nickel J H 1999 *Phys. Rev. Lett.* **82** 616
[40] Shang C H, Nowak J, Jansen R and Moodera J S 1998 *Phys. Rev.* B **58** R2917
[41] MacDonald A H, Jungwirth T and Kasner M 1998 *Phys. Rev. Lett.* **81** 705
[42] Vedyayev A, Bagrets D, Bagrets A and Dieny B 2001 *Phys. Rev.* B **63** 064429
[43] Tsymbal E Y, Burlakov V M and Oleinik I I 2002 *Phys. Rev.* B **66** 073201
[44] Han X-F, Yu A C C, Oogane M, Murai J and Daibou T 2001 *Phys. Rev.* B **63** 224404
[45] Bowen M 2002 private communication
[46] Pickett W E and Moodera J S 2001 *Phys. Today* **5** 39
[47] de Groot R A, Mueller F M, van Engen P G and Buschow K H 1983 *Phys. Rev. Lett.* **50** 2024
[48] Ishida S, Fujii S, Kawhiwagi S and Asano S 1995 *J. Phys. Soc. Japan* **64** 2152
[49] Schwarz K 1986 *J. Phys. F: Met. Phys.* **16** L211
[50] Alvarado S F, Erbudak M and Munz P 1976 *Phys. Rev.* B **14** 2740
[51] Yanase A and Siratori K 1984 *J. Phys. Soc. Japan* **53** 312
[52] Okimoto Y, Katsufuji K, Ishikawa T, Urushibara A, Arima T and Tokura Y 1995 *Phys. Rev. Lett.* **75** 109
[53] Wei J Y T, Yeh N-C and Vasques R P 1997 *Phys. Rev. Lett.* **79** 5150
[54] Mazin I I 2000 *Appl. Phys. Lett.* **77** 3000
[55] Park J H, Vescovo E, Kim H J, Kwon C, Ramesh R and Venkatesan T 1998 *Nature* **392** 794
[56] Ristoiu D, Nozières J P, Borca C N, Komesu T, Jeong H-K and Dowben P A 2000 *Europhys. Lett.* **49** 624
[57] Ji Y, Strijkers G J, Yang F Y, Chien C L, Byers J M, Anguelouch A, Xiao G and Gupta A 2001 *Phys. Rev. Lett.* **86** 5585
[58] Parker J S, Watts S M, Ivanov P G and Xiong P 2002 *Phys. Rev. Lett.* **88** 196601
[59] Lu Y, Li X W, Gong G Q, Xiao G, Gupta A, Lecoeur P, Sun J Z, Wang Y Y and Dravid V P 1996 *Phys. Rev.* B **54** R8357
[60] Viret M, Drouet M, Nassar J, Contour J P, Fermon C and Fert A 1997 *Europhys. Lett.* **39** 545
[61] Worledge D C and Geballe T H 2000 *Appl. Phys. Lett.* **76** 900
[62] Sun J Z 2001 *Physica* C **350** 215
[63] Jo M-H, Mathur N D, Evetts J E and Blamire M G 2000 *Appl. Phys. Lett.* **77** 3803
Jo M-H, Mathur N D, Todd N K and Blamire M G 2000 *Phys. Rev.* B **61** R14905
[64] Ziese M 2002 *Rep. Prog. Phys.* **65** 143
[65] Yuasa S, Sato T, Tamura E, Suzuki Y, Yamamori H, Ando K and Katayama T 2000 *Europhys. Lett.* **52** 344
[66] Callaway J and Wang C S 1977 *Phys. Rev.* B **16** 2095
[67] Moodera J S, Gallagher E F, Robinson K and Nowak J 1997 *Appl. Phys. Lett.* **70** 3050
[68] Sun J J, Soares V and Freitas P P 1999 *Appl. Phys. Lett.* **74** 448
[69] May U, Samm K, Kittur H, Hauch J, Calarco R, Rüdiger U and Güntherodt G 2001 *Appl. Phys. Lett.* **78** 2026
[70] Hagler T, Kinder R and Bayreuther G 2001 *J. Appl. Phys.* **89** 7570
[71] Seve L, Zhu W, Sinkovic B, Freeland J W, Coulthard I, Antel W J and Parkin S S P 2001 *Europhys. Lett.* **55** 439
[72] Buchanan J D R, Hase T P A, Tanner B K, Hughes N D and Hicken R J 2002 *Appl. Phys. Lett.* **81** 751
[73] Tsymbal E Y and Pettifor D G 1997 *J. Phys.: Condens. Matter* **9** L411
[74] Sugiyama M, Hayakawa J, Itou K, Asano H, Matsui M, Sakuma A and Ichimura M 2001 *J. Magn. Soc. Japan* **25** 795
[75] Sun J Z, Roche K P and Parkin S S P 2000 *Phys. Rev.* B **61** 11244
[76] Platt C L, Dieny B and Berkowitz A E 1997 *J. Appl. Phys.* **81** 5523
[77] Wulfhekel W, Klaua M, Ullmann D, Zavaliche F, Kirschner J, Urban R, Monchesky T and Heinrich B 2001 *Appl. Phys. Lett.* **78** 509
[78] Klaua M, Ullmann D, Barthel J, Wulfhekel W, Kirschner J, Urban R, Monchesky T L, Enders A, Cochran J F and Heinrich B 2001 *Phys. Rev.* B **64** 134411
[79] Bowen M, Cros V, Petroff F, Fert A, Martìnez Boubeta C, Costa-Krämer J L, Anguita J V, Cebollada A, de Teresa J M, Morellòn L, Ibarra M R, Güell F, Peirò F and Cornet A 2001 *Appl. Phys. Lett.* **79** 1655
[80] Butler W H, Zhang X-G, Schulthess T C and MacLaren J M 2001 *Phys. Rev.* B **63** 054416
[81] Platt C L, Dieny B and Berkowitz A E 1996 *Appl. Phys. Lett.* **69** 2291

[82] Gillies M F, Kuiper A E T, van Zon J B A and Sturm J M 2001 *Appl. Phys. Lett.* **78** 3496
[83] Sharma M, Nickel J H, Anthony T C and Wang S X 2000 *Appl. Phys. Lett.* **77** 2219
[84] Wang J, Cardosa S, Freitas P P, Wei P, Barradas N P and Soares J C 2001 *J. Appl. Phys.* **89** 6868
[85] Li Z, de Groot C and Moodera J S 2000 *Appl. Phys. Lett.* **77** 3630
[86] Wang J, Freitas P P, Snoeck E, Wei P and Soares J C 2001 *Appl. Phys. Lett.* **79** 4387
[87] Wang J, Freitas P P and Snoeck E 2001 *Appl. Phys. Lett.* **79** 4553
[88] Wachter P 1979 *Handbook on the Physics and Chemistry of Rare Earths* (Amsterdam: North-Holland) ch 19
[89] Mauger A and Godart C 1986 *Phys. Rep.* **141** 51
[90] Moodera J S, Hao X, Gibson G A and Meservey R 1988 *Phys. Rev. Lett.* **61** 637
Hao X, Moodera J S and Meservey R 1990 *Phys. Rev.* B **42** 8235
[91] Esaki L, Stiles P J and von Molnar S 1967 *Phys. Rev. Lett.* **19** 852
[92] LeClair P, Ha J K, Swagten H J M, Kohlhepp J T, van de Vin C H and de Jonge W J M 2002 *Appl. Phys. Lett.* **80** 625
[93] Tedrow P M and Meservey R 1975 *Solid State Commun.* **16** 71
[94] Moodera J S, Taylor M E and Meservey R 1989 *Phys. Rev.* B **40** R11980
[95] Parkin S S P 1998 *US Patent Specification* 5,764,567
[96] Sun J J and Freitas P P 1999 *J. Appl. Phys.* **85** 5264
[97] Appelbaum J A and Brinkman W F 1969 *Phys. Rev.* **186** 464
Appelbaum J A and Brinkman W F 1970 *Phys. Rev.* B **2** 907
[98] Moodera J S, Kim T H, Tanaka C T and de Groot C H 2000 *Phil. Mag.* B **80** 195
[99] Vedyayev A, Ryzhanova N, Lacroix C, Giacomoni L and Dieny B 1997 *Europhys. Lett.* **39** 219
[100] Mathon J and Umerski A 1999 *Phys. Rev.* B **60** 1117
[101] Yuasa S, Nagahama T and Suzuki Y 2002 *Science* **297** 234
[102] Barnaś J and Fert A 1998 *Phys. Rev. Lett.* **80** 1058
[103] Takahashi S and Maekawa S 1998 *Phys. Rev. Lett.* **80** 1758
[104] Majumdar K and Hershfield S 1998 *Phys. Rev.* B **57** 11521
[105] Imamura H, Takahashi S and Maekawa S 1999 *Phys. Rev.* B **59** 6017
[106] Brataas A, Nazarov Yu V, Inoue J and Bauer G E W 1999 *Phys. Rev.* B **59** 93
[107] Schelp L F, Fert A, Fettar F, Holody P, Lee S F, Maurice J L, Petroff F and Vaurès A 1997 *Phys. Rev.* B **56** R5747
[108] Mitani S, Takahashi S, Takanashi K, Yakushiji Y, Maekawa S and Fujimori H 1998 *Phys. Rev. Lett.* **81** 2799
[109] Zhu T and Wang Y J 1999 *Phys. Rev.* B **60** 11918
[110] Yakushiji K, Mitani S, Takanashi K, Takahashi S, Maekawa S, Imamura H and Fujimori H 2001 *Appl. Phys. Lett.* **78** 515
[111] Yakushiji K, Mitani S, Takanashi K and Fujimori H 2002 *J. Appl. Phys.* **91** 7038
[112] Landauer R 1988 *IBM J. Res. Dev.* **32** 306
Büttiker M 1988 *IBM J. Res. Dev.* **32** 317
[113] MacLaren J M, Zhang X-G and Butler W H 1997 *Phys. Rev.* B **56** 11827
[114] Zhang S and Levy P M 1998 *Phys. Rev. Lett.* **81** 5660
[115] Wilczynski M and Barnaś J 2000 *J. Appl. Phys.* **88** 5230
[116] Zhang X D, Li B Z, Sun G and Pu F C 1997 *Phys. Rev.* B **56** 5484
[117] Sheng L, Chen Y, Teng H Y and Ting C S 1999 *Phys. Rev.* B **59** 480
[118] Chshiev M, Stoeffler D, Vedyayev A and Ounadjela K 2002 *Europhys. Lett.* **58** 257
[119] Zhang S and Levy P M 1999 *Eur. Phys. J.* B **10** 599
[120] Zhao B, Mönch I, Mühl T, Vinzelberg H and Schneider C M 2002 *J. Appl. Phys.* **91** 7026
[121] Itoh H and Inoue J 2001 *Surf. Sci.* **493** 748
[122] Tsymbal E Y, Oleinik I I and Pettifor D G 2000 *J. Appl. Phys.* **87** 5230
[123] de Boer P K, de Wijs G A and de Groot R A 1998 *Phys. Rev.* B **58** 15422
[124] Oleinik I I, Tsymbal E Y and Pettifor D G 2002 *Phys. Rev.* B **65** 020401
[125] Oleinik I I, Tsymbal E Y and Pettifor D G 2000 *Phys. Rev.* B **62** 3952
[126] MacLaren J M, Zhang X-G, Butler W H and Wang X 1999 *Phys. Rev.* B **59** 5470
[127] Mavropoulos Ph, Papanikolaou N and Dederichs P H 2000 *Phys. Rev. Lett.* **85** 1088
[128] Mathon J and Umerski A 2001 *Phys. Rev.* B **63** 220403
[129] Mathon J 1997 *Phys. Rev.* B **56** 11810
[130] Meyerheim H L, Popescu R, Jedrecy N, Vedpathak M, Sauvage-Simkin M, Pinchaux R, Heinrich B and Kirschner J 2002 *Phys. Rev.* B **65** 144433
[131] Gustavsson F, George J M, Etgens V H and Eddrief M 2001 *Phys. Rev.* B **64** 184422
[132] Cardosa S, Freitas P P, de Jesus C, Wei P and Soares J C 2000 *Appl. Phys. Lett.* **76** 610

[133] Sun J J, Shimazawa K, Kasahara N, Sato K, Saruki S, Kagami T, Redon O, Araki S, Morita H and Matsuzaki M 2000 *Appl. Phys. Lett.* **76** 2424

[134] Schmalhorst J, Bruckl H, Justus M, Thomas A, Reiss G, Vieth M, Gieres G and Wecker J 2001 *J. Appl. Phys.* **89** 586

[135] Da Costa V, Tiusan C, Dimopoulos T and Ounadjela K 2000 *Phys. Rev. Lett.* **85** 876
Da Costa V, Henry Y, Bardou F, Romeo M and Ounadjela K 2000 *Eur. Phys. J.* B **13** 297

[136] Bratkovsky A M 1997 *Phys. Rev.* B **56** 2344
Bratkovsky A M 1998 *Appl. Phys. Lett.* **72** 2334

[137] Itoh H, Inoue J, Maekawa S and Bruno P 1999 *J. Magn. Magn. Mater.* **199** 545

[138] Tsymbal E Y and Pettifor D G 1998 *Phys. Rev.* B **58** 432
Tsymbal E Y and Pettifor D G 1999 *J. Magn. Magn. Mater.* **199** 146
Tsymbal E Y and Pettifor D G 1999 *J. Appl. Phys.* **85** 5801

[139] Jansen R and Lodder J C 2000 *Phys. Rev.* B **61** 5860

[140] Inoue J, Nishimura N and Itoh H 2002 *Phys. Rev.* B **65** 104433

[141] Levy P M, Wang K S, Dederichs P H, Heide C, Zhang S F and Szunyogh L 2002 *Phil. Mag.* B **82** 763

[142] Uiberacker C and Levy P M 2002 *Phys. Rev.* B **65** 169904

[143] Bagrets D, Bagrets A, Vedyayev A and Dieny B 2002 *Phys. Rev.* B **65** 064430

[144] Wunnicke O, Papanikolaou N, Zeller R, Dederichs P H, Drchal V and Kudrnovsky J 2002 *Phys. Rev.* B **65** 064425

[145] Tsymbal E Y 2001 unpublished

[146] Tsymbal E Y, Sokolov A, Sabirianov I F and Doudin B 2003 submitted

[147] Doudin B, Gilbert S, Redmond G and Ansermet J-Ph 1997 *Phys. Rev. Lett.* **79** 933

[148] Rippard W H, Perrella A C and Buhrman R A 2001 *Appl. Phys. Lett.* **78** 1601

[149] Tsymbal E Y and Pettifor D G 2001 *Phys. Rev.* B **64** 212401

[150] Parkin S S P, Roche K P, Samant M G, Rice P M, Beyers R B, Scheuerlein R E, O'Sullivan E J, Brown S L, Bucchigano J, Abraham D W, Lu Yu, Rooks M, Trouilloud P L, Wanner R A and Gallagher W J 1999 *J. Appl. Phys.* **85** 5828

[151] Heide C and Elliott R J 2000 *Europhys. Lett.* **50** 271
Heide C, Elliott R J and Wingreen N S 1999 *Phys. Rev.* B **59** 4287

[152] Skomski R and Dowben P A 2002 *Europhys. Lett.* **58** 544

[153] Kikkawa J M and Awschalom D D 1999 *Nature* **397** 139

[154] Fiederling R, Keim M, Reuscher G, Ossau W, Schmidt G, Waag A and Molenkamp L W 1999 *Nature* **402** 787

[155] Ohno Y, Young D K, Beschoten B, Matsukura F, Ohno H and Awschalom D D 1999 *Nature* **402** 790

[156] Zhu H J, Ramsteiner M, Kostial H, Wassermeier M, Schönherr H-P and Ploog K H 2001 *Phys. Rev. Lett.* **87** 016601

[157] Hanbicki A T, Jonker B T, Itskos G, Kioseoglou G and Petrou A 2002 *Appl. Phys. Lett.* **80** 1240

[158] Tanaka M and Higo Y 2001 *Phys. Rev. Lett.* **87** 026602

[159] Hirohata A, Steinmueller S J, Cho W S, Xu Y B, Guertler C M, Wastlbauer G, Bland J A C and Holmes S N 2002 *Phys. Rev.* B **66** 035330

[160] Garcia N, Munoz M and Zhao Y-W 1999 *Phys. Rev. Lett.* **82** 2923

[161] Bruno P 1999 *Phys. Rev. Lett.* **83** 2425

[162] Tatara G, Zhao Y-W, Munoz M and Garcia N 1999 *Phys. Rev. Lett.* **83** 2030

[163] Chopra H D and Hua S Z 2002 *Phys. Rev.* B **66** R020403

[164] Rabson D A, Jönsson-Akerman B J, Romero A H, Escudero R, Leighton C, Kim S and Schuller I K 2001 *J. Appl. Phys.* **89** 2786

[165] Munoz M, Qian G G, Karar N, Cheng H, Saveliev I G, Garcia N, Moffat T P, Chen P J, Gan L and Egelhoff W F 2001 *Appl. Phys. Lett.* **79** 2946

[166] Filip A T, LeClair P, Smits C J P, Kohlhepp J T, Swagten H J M, Koopmans B and de Jonge W J M 2002 *Appl. Phys. Lett.* **81** 1815